

Field theory for generalized Shastry-Sutherland models

David Carpentier

Institute for Theoretical Physics, University of California, Santa Barbara, CA 93106
and

CNRS-Laboratoire de Physique de l'ENS-Lyon, 46 Allée d'Italie, 69007 Lyon, France

Leon Balents

Physics Department, University of California, Santa Barbara, CA 93106

(November 7, 2018)

We consider the bosonic dimer representation for *Generalized Shastry-Sutherland models* that have the same symmetries as the original Shastry-Sutherland model and preserve the exact dimer eigenstate. Various phases with differing types of magnetic order are found within mean-field theory for the corresponding low-energy effective dimer field theory. Transitions are allowed between any of these mean-field phases, which are *dimer bose condensates*, and with the dimer phase, which is the *dimer bose vacuum*. The Néel state, absent from this mean-field study, is described as a bosonic Mott insulator induced by the coupling to the underlying lattice. Moreover, dimer bose condensates with *local* Néel order are found to be unstable to spiral states. Instead of a direct phase transition between the dimer and the Néel phases, we propose an intermediate weakly incommensurate spin-density wave (WISDW) phase. The stability of the mean-field transitions is studied by renormalization techniques in $d = 2$, the upper critical dimension. While the transition from the Néel phase is found to be stable, the transition point from the dimer phase is not perturbatively accessible. We argue that the latter renormalization results point to the possibility of an intermediate phase of a different kind.

75.10.Jm, 75.30.Kz, 64.70.Rh.

I. INTRODUCTION

The Shastry-Sutherland (SS) model¹ is a remarkable two-dimensional (2D) analog of the Majumdar-Gosh spin chain², possessing an exact dimerized eigenstate, despite non-trivial spin-spin interactions. It recently received much attention³⁻⁶ due to its relevance for the description of the quasi-two dimensional compound⁷ $\text{SrCu}_2(\text{BO}_3)_2$. The original model is described by the Hamiltonian⁸

$$H_{SS} = J_1 \sum_{\langle i,j \rangle} \vec{S}_i \cdot \vec{S}_j + J_2 \sum_{\langle\langle k,l \rangle\rangle} \vec{S}_k \cdot \vec{S}_l, \quad (1)$$

where J_1 is the coupling along the solid lines of figure 1, and J_2 along the dashed bonds. As both interaction terms couple the two spins of each dimer (solid bond in Fig. 1) *symmetrically*, the dimerized state (direct-product of singlet states on each dimer) is an exact eigenstate of the hamiltonian (1) for any value of J_1 and J_2 .

In this paper, we will also consider the three-dimensional (3D) extension of the SS model⁶, relevant to the description of the $\text{SrCu}_2(\text{BO}_3)_2$ compound. This 3D model is defined on a 3D lattice consisting of a stack of alternate 2D SS lattices (see Fig.1 : every other layer in the z direction is rotated by $\pi/2$). The spins of dimers lying on top of each other interact via an additional coupling,

$$H_{3d} = J_3 \sum_z \sum_{\langle i,j \rangle} \vec{S}_{i,z} \cdot \vec{S}_{j,z+1}, \quad (2)$$

where i, j span the spins of the two dimers on top of each other (see Fig. 1). The dimerized SS is also an exact eigenstate of this generalization.

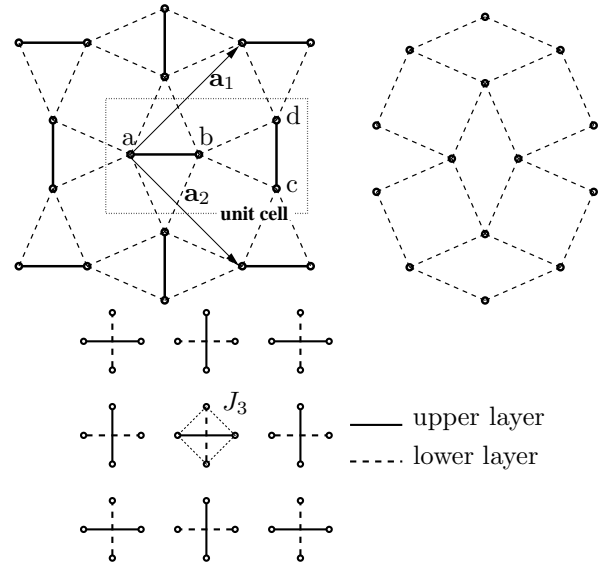


FIG. 1. Topology of the lattice defining the Shastry-Sutherland model (top left). The right lattice, equivalent to a square lattice, corresponds to the situation where $J_1 = 0$. The bottom figure shows the spatial configuration of the layers in the 3D version of the Shastry-Sutherland model.

The ground state of the SS model is known in the two extreme limits. For $J_2 = 0$, the dimers are completely decoupled from each other and the above SS dimer state is obviously the ground state. As all other states have an excitation energy of order J_1 , we expect the SS dimer state to remain the ground state for small $J_2 \ll J_1$. On the other hand for $J_1 = 0$, the SS model becomes equivalent to the Heisenberg model with the exchange coupling J_2 defined on a square lattice as can be seen on Fig.1 (right upper part). In this limit the ground state is a Néel state, possessing staggered magnetization⁹ (on the underlying square lattice). The additional J_1 interaction in this picture corresponds to a staggered diagonal exchange introduced in half the plaquettes. This dimerization *quadruples* the unit cell, which thus contains four spins. A convenient choice of unit cell is shown in Fig.1. For $J_1 \ll J_2$, the Néel state is expected to persist, as can be verified in perturbation theory⁴. The SS model is thus expected to have an “antiferromagnetic” (in the square lattice sense) ground state for $J_2/J_1 > \mathcal{J}'_c$ and the exact dimerized ground state for $J_2/J_1 < \mathcal{J}_c \leq \mathcal{J}'_c$. The intervening range has been investigated by a number of authors^{10,3,4}. Various numerical methods^{4,3} suggest that $\mathcal{J}_c \approx \mathcal{J}'_c \approx 0.69$, and possibly a direct transition between the two states. Series expansions about the dimer limit show a vanishing of the triplet excitation gap very close to this point, and a second-order transition of some type was suggested. Possible intermediate spiral phases were discussed within a mean-field slave boson approach¹⁰.

The purpose of the present paper is to propose a new framework to investigate the transitions and possible phases of *generalized Shastry-Sutherland* (GSS) models in 2D and 3D. By *generalized Shastry-Sutherland* models we mean spin Hamiltonians defined on the same lattice as the original SS model (Fig.1), but with general local interactions that satisfy two conditions: (1) the SS dimer state remains an exact eigenstate of the model, and (2) the symmetries of the SS model are maintained. To study the phases of these models, we take the SS dimer state as a starting point, and construct a field theory perturbatively around it. The underlying idea of our approach is the following : as the SS dimer state is an exact non-critical eigenstate, if the system was undergoing a second-order quantum phase transition from it, the ground-state would be non-critical on one side of the transition. The similarity between this scenario and the two-dimensional superfluid-insulator transition¹¹ motivates the introduction of a *bosonic dimer spin representation* which is done in section II. This method represents the four states of a pair of spins by the vacuum and three singly-occupied states of a triplet of hard-core “dimer-bosons”. The GSS spin model is then exactly translated into a square lattice boson model with complex interactions, whose boson vacuum corresponds to the SS dimer state.

Focusing on the universal properties of the possible transitions of this bosonic model, we derive the corresponding low-energy, long wavelength effective dimer field theory (DFT). In constructing this field theory, we

assume that all ordering occurs for small crystal momentum k on the scale of the Brillouin zone, i.e. $ka \ll 1$, where a is the lattice spacing. Because of the four-site unit cell, this includes *both* the Néel and dimer states, neither of which breaks the translational symmetry of the SS lattice. The upper critical dimension of this new DFT is found to be $d = 2$. Hence, in a sufficiently three dimensional material, the phases of the GSS model can be described within a Mean-Field Theory (MFT). The phases captured within this mean-field approach, which correspond to various coherent *condensates* of the dimer bosons, are described in section III A 1. Due to the intrinsic complexity of the DFT, the mean-field description is carried on a simpler 2D “sub-model” whose analysis contains the necessary phases. Besides the dimer state, several phases with interesting local magnetic order are found within this approach : (i) an antiparallel phase where on each dimer the spins arrange in an antiparallel way, (ii) a chiral phase where these spins rotate with respect to each other within a bond but the average magnetization vanishes, and (iii) a spiral phase with both non-zero magnetization and chirality. Mean field theory predicts continuous transitions between all these phases except between the chiral and the spiral phases, connected by a first-order transition.

Surprisingly, *none* of these Bose condensates corresponds to the antiferromagnetic (on the associated square lattice) phase! On the contrary, we show that (for the full set of GSS models), if the quantum phase transition out of the dimerized state can be regarded as Bose condensation (even if it is *first order*), the resulting ordered state *cannot* have Néel order without fine-tuning of parameters. The closest such a Bose condensate can approach the antiferromagnet is to sustain weakly *incommensurate* spin-density wave (WISDW) order (i.e. a periodic modulation of the expectation value of the total spin on each dimer) at a wavevector near but not equal to (π, π) on the underlying square lattice. Moreover, even such a WISDW state necessarily contains concomitant transverse (to the local WISDW quantization axis) magnetic (e.g. antiparallel) and chiral order. These two properties follow from symmetry considerations. In particular, the total spin on each dimer is invariant under spatial reflections, and hence must be bilinear in the Bose fields. Moreover, since it is an SU(2) vector, it can only be related to a cross-product of these fields, which must themselves therefore have non-zero values along the two transverse axes. The latter condition implies spontaneously broken reflection and (four-fold) rotational symmetry, and full breaking of SU(2) symmetry (i.e. with no remaining invariant subgroups). These conditions lead to a generic long-wavelength instability of the gapless magnon (Goldstone) modes of the broken SU(2) to incommensurate ordering.

The upshot is that to describe the ordinary antiferromagnet, with commensurate Néel order and no transverse magnetic ordering, it is necessary to go beyond the simplest DFT and include the couplings between the dimer

bosons and the underlying lattice. We show that, in this context, the antiferromagnetic phase is described not as a Bose condensate but as a bosonic Mott insulator. The failure of mean-field theory to describe such a Mott insulator can be understood from the uncertainty principle. Because the Mott insulator is a state with “definite” boson number, the strong fluctuations of the conjugate boson phase invalidate the mean-field approach. Simple arguments then show that a direct continuous transition from this antiferromagnetic phase to the dimer SS state is not possible.

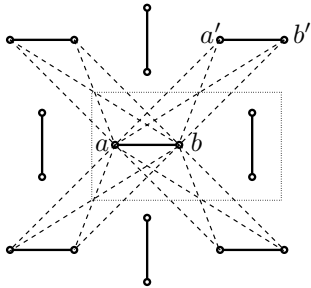


FIG. 2. Four-spin interaction that is *exactly* equivalent to a dimer-boson hopping term. The dashed lines illustrate interactions between the a and b spins of neighboring unit cells (see Eq. 3). There are identical interactions, rotated by forty-five degrees, between the c and d spins (not shown).

Instead, in three dimensions the theory suggests it is possible to cross from the Dimer to Néel states via an *intermediate* Bose condensate in a sequence of continuous transitions. At the first transition the dimer Bosons condense to form a WISDW state. Upon further varying some parameter in the theory, the mean density of dimer bosons approaches one per dimer, and the system undergoes a *superfluid-insulator-like* transition to the bosonic Mott insulator which corresponds to the Néel state. While there is no numerical evidence for this two-stage transition in the usual SS model, it should occur naturally in other models in the GSS class. The dimer-boson representation gives strong hints as to the nature of the additional interactions that should be added to the SS model in order to facilitate such a two-step transition. In particular, by a judicious choice of *four-spin* interactions, the *kinetic energy* of the dimer-bosons can be explicitly increased. This is accomplished by the following term, illustrated in Fig. 2:

$$H^* = -J^* \sum_{\langle \mathbf{x}\mathbf{x}' \rangle} \left[\frac{1}{2} (\vec{S}_a - \vec{S}_b) \cdot (\vec{S}_{a'} - \vec{S}_{b'}) + 2(\vec{S}_a \times \vec{S}_b) \cdot (\vec{S}_{a'} \times \vec{S}_{b'}) + (aba'b' \leftrightarrow cdc'd') \right], \quad (3)$$

where the subscripts, $abcd, a'b'c'd'$, indicate the appropriate spin in the unit cell centered on \mathbf{x}, \mathbf{x}' , respectively. The sum is taken over nearest-neighbor unit cells, i.e. all pairs of lattice vectors satisfying $\mathbf{x} - \mathbf{x}' = \pm \mathbf{a}_1, \pm \mathbf{a}_2$, where $\mathbf{a}_{1,2}$ are the primitive vectors shown in Fig. 1.

Remarkably, this rather strange interaction can be exactly rewritten, using the formulae in section II, as a simple nearest-neighbor dimer-boson hopping term. It therefore preserves the exact dimer eigenstate. In the original SS model $J^* = 0$, and the boson kinetic energy arises only through high-order virtual processes involving many J_2 exchanges. By explicitly including it, $H_{SS} \rightarrow H_{GSS} = H_{SS} + H^*$, the bosons acquire a “bare” kinetic energy and Bose condensate is rendered more favorable – indeed if J^* is increased and a low density of bosons maintained by simultaneously increasing J_1 , the transition out of the dimer state becomes parametrically better described as condensation of a dilute, weakly-interacting Bose gas. A possible schematic phase diagram showing the evolution of the ground state of the GSS model on increasing J^* in three dimensions is indicated in Fig. 3a.

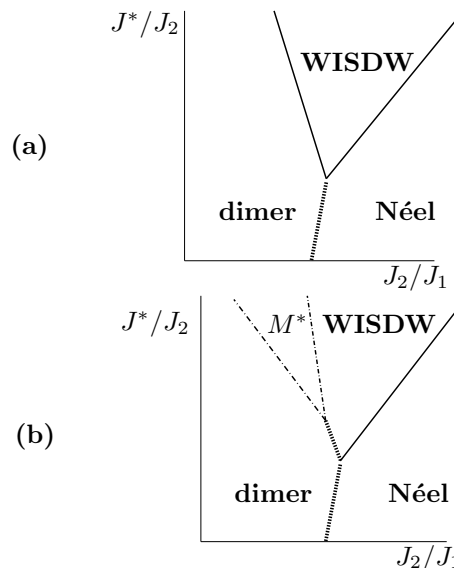


FIG. 3. Schematic zero-temperature phase diagrams for GSS models upon increasing a parameter, such as J^* , that favors dimer-boson condensation in (a) three dimensions, (b) two dimensions. In three dimensions, only the dimer, Néel, and Weakly Incommensurate Spin Density Wave (WISDW) states need be present. In two dimensions, fluctuation effects may open up a magnetically fractionalized region M^* between the dimer and WISDW states. Thick (hashed) lines indicate first-order transitions, thin solid lines second-order transitions, and dot-dashed lines transitions of unknown order.

Finally, we come back to the two-dimensional GSS models, and consider the effect of critical fluctuations whose description is crucial at the upper critical dimension. The natural framework to study these fluctuations is provided by the renormalization group (RG) : in that context, fluctuations correspond to either marginally irrelevant or relevant operators in $d = 2$. We derive the one loop RG equations for both the general DFT (bose-condensate transitions) and the field theory describing the transition from the Néel state to the WISDW phase.

For this latter transition, the ‘gaussian’ fixed point is found to be stable for a range of parameters. This shows that fluctuations do not destabilize the transition suggested by the mean-field behaviour, as shown in Fig.3. For the full DFT, which contains additional cubic terms allowed by the existence of non-collinear order parameters, we have studied the RG flow numerically and analytically. All our approaches to the analysis of the RG equations were consistent with a run-away flow of the coupling constants. This situation corresponds to marginally relevant perturbations at the gaussian fixed point. This suggests a different scenario in 2D than the MFT description of the 3D GSS models (Fig.3).

It is tempting to connect the fluctuation-dominated regime near the mean-field critical point with earlier theories of “quantum-disordered” non-collinear magnetic states.¹² In particular, it has been suggested that models with *classically* incommensurate non-collinear order may instead exhibit exotic “fractionalized” quantum paramagnets in the presence of strong quantum fluctuations (e.g. for sufficiently small spin and/or frustrated interactions). This conclusion is based on analysis of sigma models in which *local* (in space and time) non-collinear order is assumed, but that the orientation of this non-collinear order parameter fluctuates quantum-mechanically. The “run-away” flows in the RG treatment suggest such a description might apply. First, the RG instability is driven by novel *cubic interaction terms* that are non-zero only for non-collinear spin configurations, and present in the GSS model due to its unusual symmetries. Further, these run-away flows lead to a large fluctuation-induced “critical point shift”, so that the true critical point occurs deep within the regime in which a local order-parameter amplitude is established. A possible interpretation of our RG results is therefore that the mean-field WISDW state in the vicinity of the critical regime is replaced by such a fractionalized phase. Such fractionalized states have a number of remarkable properties^{12,13} (topological order, deconfined spin-1/2 excitations, etc.), which make this an exciting possibility. Notably, the presence of a continuous quantum phase transition from the dimer state to a fractionalized quantum paramagnet has been suggested recently by Marston *et. al.* using completely different large- N methods.¹⁷ Our approach does not allow us to address the *order* of such a putative quantum critical point. A schematic phase diagram for the two-dimensional case is shown in Fig. 3b.

The remainder of the paper is organized as follows. In Sec. II, we introduce the dimer-boson representation and write down the general DFT allowed for GSS models in coarse-grained variables. We also show how this general DFT reduces to a “sub-model” if an explicit bond-alternation is added to the GSS model to break 90-degree rotational symmetry. In Sec. III, we discuss the structure of the mean-field limit of the DFT, determining the full phase diagram for the sub-model, and describing the types of ordering in the general DFT. We also prove that for the general DFT a generic Bose condensate with local

Néel order is unstable to a weakly incommensurate spiral (WISDW). In Sec. IV, we show how a true antiferromagnet with commensurate $((\pi, \pi))$ Néel order and no other broken symmetries is described as a Mott insulator, and determine the effective field theory for the AF-WISDW transition. Finally, in Sec. V we analyze the effect of quantum fluctuations in two dimensions using the RG, both for the AF-WISDW and the dimer-WISDW critical points (or more generally transitions out of the dimer state into Bose condensates). Details of the RG calculations are given in an appendix.

II. MODELS AND BOND-OPERATOR REPRESENTATION

A. Generalized Shastry-Sutherland models and Dimer Field theories

In this paper, we explore the behavior of *Generalized* SS (GSS) models using a *Dimer Field Theory* (DFT). By GSS, we consider in a general manner any model having the same symmetries as the SS Hamiltonian (see below), preserving the exact ground state, and without long-range (i.e. power-law) interactions. The DFT of such models is obtained in two stages. First, the original spin model is rewritten in terms of triplet bond operators. As pointed out originally in Ref. 14,¹⁵ a pair of spins can be represented *exactly* by a triplet of hard-core bosons. Hence

$$\vec{S}_a(\mathbf{x}) = \frac{1}{2} \left[\vec{b}_{1\mathbf{x}} + \vec{b}_{1\mathbf{x}}^\dagger + i\vec{b}_{1\mathbf{x}}^\dagger \times \vec{b}_{1\mathbf{x}} \right], \quad (4a)$$

$$\vec{S}_b(\mathbf{x}) = \frac{1}{2} \left[-\vec{b}_{1\mathbf{x}} - \vec{b}_{1\mathbf{x}}^\dagger + i\vec{b}_{1\mathbf{x}}^\dagger \times \vec{b}_{1\mathbf{x}} \right], \quad (4b)$$

$$\vec{S}_c(\mathbf{x}) = \frac{1}{2} \left[\vec{b}_{2\mathbf{x}} + \vec{b}_{2\mathbf{x}}^\dagger + i\vec{b}_{2\mathbf{x}}^\dagger \times \vec{b}_{2\mathbf{x}} \right], \quad (4c)$$

$$\vec{S}_d(\mathbf{x}) = \frac{1}{2} \left[-\vec{b}_{2\mathbf{x}} - \vec{b}_{2\mathbf{x}}^\dagger + i\vec{b}_{2\mathbf{x}}^\dagger \times \vec{b}_{2\mathbf{x}} \right], \quad (4d)$$

is an exact rewriting of the original spin operators in terms of bosons, $[b_{i\mathbf{x}}, b_{j\mathbf{x}'}^\dagger] = \delta_{ij}\delta_{\mathbf{x}\mathbf{x}'}$, provided the hard-core constraint,

$$\vec{b}_{1\mathbf{x}}^\dagger \cdot \vec{b}_{1\mathbf{x}}, \vec{b}_{2\mathbf{x}}^\dagger \cdot \vec{b}_{2\mathbf{x}} = 0, 1, \quad (5)$$

is enforced. A third useful relation, that will be used later in this paper, can be deduced from the above definitions (4) with the constraint (5). It expresses the chirality on each bond :

$$2 \vec{S}_a \times \vec{S}_b = i(\vec{b}_{1\mathbf{x}}^\dagger - \vec{b}_{1\mathbf{x}}). \quad (6)$$

A general Hamiltonian for a GSS model can thus be rewritten as a local model of interacting bosons via Eqs. 4-5. This bond-operator representation is particularly useful for GSS models in that it captures the dimer eigenstate in the simplest possible way – as the

boson vacuum. The representation becomes awkward in the original SS model when $J_2 \gg J_1$, in which the 2D square-lattice Heisenberg model is approached. This is because the canonical transformation in Eqs. 4-5, while exact, does not respect the space-group symmetries of the square lattice. Away from this limit, however, all the *physical* symmetries remain explicit.

Using Eqs. (4-5), any interaction between hard-core bosons can also be inverted and rewritten in terms of the original spins. It is particularly illuminating to rewrite the four-spin interaction in Eq. (3),

$$H^* = -J^* \sum_{(\mathbf{x}\mathbf{x}')} \sum_{i=1,2} \left(\vec{b}_{i\mathbf{x}}^\dagger \cdot \vec{b}_{i\mathbf{x}'} + \text{h.c.} \right), \quad (7)$$

which becomes a simple boson hopping term. Formally, although we do not explore this route in detail, J^* introduced in this manner can act as a control parameter for the dimer boson theory. In particular, as J^* is increased, the boson kinetic energy becomes dominant, and the system is better and better approximated as a weakly-interacting Bose gas. For such a gas, the Bose condensate approximation to the interacting ground state is obviously very good.

Next, we adopt a *coarse-grained* effective field theory point of view. In particular, we will assume that any ordering and/or low-energy fluctuations in the system at most weakly (i.e. at very long wavelengths) breaks lattice translational symmetry. By translational symmetry, we mean translation by a Bravais lattice vector $\mathbf{x} = n_1 \mathbf{a}_1 + n_2 \mathbf{a}_2$, with integer n_1, n_2 and $\mathbf{a}_{1,2}$ indicated in Fig. 1. Note that because of the rather large four-site unit cell, this requirement is not very restrictive. In particular, both the dimer and Néel order are translationally invariant in this strict sense.

The quadratic terms are

$$S^{(2)} = \int_{\mathbf{x},\tau} \left\{ \vec{\phi}_1^* [Z \partial_\tau + r - c_1 \partial_x^2 - c_2 \partial_y^2] \vec{\phi}_1 + \vec{\phi}_2^* [Z \partial_\tau + r - c_2 \partial_x^2 - c_1 \partial_y^2] \vec{\phi}_2 - d \left(\vec{\phi}_1^* \partial_x \partial_y \vec{\phi}_2 + \vec{\phi}_2^* \partial_x \partial_y \vec{\phi}_1 \right) \right\}. \quad (8a)$$

The cubic terms may be written

$$S^{(3)} = i \int_{\mathbf{x},\tau} \left\{ \left[g_0 \vec{\phi}_1^* \cdot \partial_x \vec{\phi}_1 \times \vec{\phi}_1 + g_1 \vec{\phi}_2^* \cdot \partial_x \vec{\phi}_1 \times \vec{\phi}_2 + g_2 \vec{\phi}_1^* \cdot \partial_x \vec{\phi}_2 \times \vec{\phi}_2 + g_4 \vec{\phi}_2^* \cdot \partial_x \vec{\phi}_2 \times \vec{\phi}_1 - \text{h.c.} \right] + [y \leftrightarrow x, 1 \leftrightarrow 2] \right\}, \quad (8b)$$

where the product (\times) indicates the (vector)cross-product. Finally, the allowed quartic terms are

$$S^{(4)} = \int_{\mathbf{x},\tau} \left\{ u_1 \left[(\vec{\phi}_1^* \cdot \vec{\phi}_1)(\vec{\phi}_1^* \cdot \vec{\phi}_1) + 1 \leftrightarrow 2 \right] + 2u_2 \left[(\vec{\phi}_1^* \cdot \vec{\phi}_1)(\vec{\phi}_2^* \cdot \vec{\phi}_2) \right] + u_3 \left[(\vec{\phi}_1^* \cdot \vec{\phi}_2)(\vec{\phi}_1^* \cdot \vec{\phi}_2) + 1 \leftrightarrow 2 \right] + 2u_4 \left[(\vec{\phi}_1^* \cdot \vec{\phi}_2)(\vec{\phi}_2^* \cdot \vec{\phi}_1) \right] \right. \\ \left. + v_1 \left[(\vec{\phi}_1^* \cdot \vec{\phi}_1)(\vec{\phi}_1^* \cdot \vec{\phi}_1^*) + 1 \leftrightarrow 2 \right] + v_2 \left[(\vec{\phi}_2^* \cdot \vec{\phi}_2)(\vec{\phi}_1^* \cdot \vec{\phi}_1^*) + 1 \leftrightarrow 2 \right] + 4v_3 \left[(\vec{\phi}_1^* \cdot \vec{\phi}_2)(\vec{\phi}_1^* \cdot \vec{\phi}_2^*) \right] \right. \\ \left. + w_1 \left[(\vec{\phi}_1^* \cdot \vec{\phi}_1)(\vec{\phi}_1^* \cdot \vec{\phi}_1^*) + 1 \leftrightarrow 2 \right] + w_2 \left[(\vec{\phi}_2^* \cdot \vec{\phi}_2)(\vec{\phi}_1^* \cdot \vec{\phi}_1^*) + 1 \leftrightarrow 2 \right] + 4w_3 \left[(\vec{\phi}_1^* \cdot \vec{\phi}_2)(\vec{\phi}_2^* \cdot \vec{\phi}_1^*) + 1 \leftrightarrow 2 \right] + \text{h.c.} \right\}. \quad (8c)$$

With this assumption, we can imagine formally integrating out (in the path-integral sense) the degrees of freedom (Fourier modes of the b_i, b_i^\dagger operators) with wavevectors $|\mathbf{q}| > \Lambda$, where $\Lambda \ll \pi$ is a cut-off defining a sphere around the origin in momentum space. This procedure defines an (approximate) continuum limit, $\vec{b}_{i\mathbf{x}} \rightarrow \vec{\phi}_i(\mathbf{x})$, $\vec{b}_{i\mathbf{x}}^\dagger \rightarrow \vec{\phi}_i^*(\mathbf{x})$, with a pair of continuum triplet fields $\vec{\phi}_i, \vec{\phi}_i^*$. Because these continuum fields are effectively averages of the microscopic bosons over many unit cells, this coarse-graining relaxes the hard-core constraint. Thus we arrive at an effective “soft spin” field theory.

In practice, for a general GSS Hamiltonian, it is impossible to integrate out the short-wavelength modes explicitly. Instead, in the spirit of classical Landau theory, we use the constraints of symmetry and the presence of an exact dimer ground state to determine the form of the long-wavelength effective action in an expansion in powers of the fields and in space-time gradients. Beside the invariance by time-reversal, the symmetries of the initial SS model (and by extension of the GSS models we consider) can be determined by inspection of the geometry of the corresponding lattice (Fig. 1) :

- Time reversal : $\vec{S} \rightarrow -\vec{S}$; $\vec{\phi}_a \rightarrow -\vec{\phi}_a^*$; $\tau \rightarrow -\tau$
- $\pi/2$ rotation : $\vec{\phi}_1 \rightarrow \vec{\phi}_2$; $\vec{\phi}_2 \rightarrow -\vec{\phi}_1$; $x \rightarrow y$; $y \rightarrow -x$
- Reflection with respect to x : $x \rightarrow -x$; $\vec{\phi}_1 \rightarrow -\vec{\phi}_1$
- Reflection with respect to y : $y \rightarrow -y$; $\vec{\phi}_2 \rightarrow -\vec{\phi}_2$

We keep terms up to fourth order in the fields and second order in spatial gradients. Breaking up the effective action by powers of the fields gives $S = S^{(2)} + S^{(3)} + S^{(4)}$.

Eqs. 8 embody numerous unique features of the GSS models. For $r > 0$, the quadratic action $S^{(2)}$ in Eq. 8a indicates the presence of a gap of order r for triplet excitations. For r sufficiently positive, the ground state of the system is the boson vacuum, corresponding to the exact dimer eigenstate. Neglecting for the moment the cubic and quartic terms, as $r \rightarrow 0$ the gap for triplet excitations vanishes. At this (mean-field) critical point ($r = 0$), the space-time scaling is highly anisotropic: naively, $\omega \sim k^z$ with the dynamical exponent $z = 2$. This strongly anisotropic scaling is very different from the $z = 1$ behavior expected at a generic $O(3)$ transition described by, e.g. the non-linear sigma model. This anisotropy is due to the fluctuationless nature of the dimer state and consequent reduction of “quantum fluctuations” near the putative critical point.

A further constraint on Eqs. 8 due to the presence of the exact dimer state is the absence of “anomalous” terms involving products *only* of creation or annihilation operators. For instance, consider the introduction of an exchange coupling between a and b spins in *different* unit cells, which destroys the exactness of the dimer state. This interaction leads directly to an anomalous term of the form $J''(\vec{\phi}_i \cdot \vec{\phi}_i + \text{c.c.})$, which induces a cross-over to more conventional $z = 1$ behavior.

An unusual feature of the above effective action is the cubic terms in Eq. 8b. The presence of such cubic invariants involving single spatial gradients is a unique feature of the GSS models. They are allowed by symmetry due to a combination of factors: first, the complex nature of the triplet $\vec{\phi}_i$ fields, (corresponding to non-linear order parameters in the vertical and horizontal directions) makes it possible to construct a non-vanishing triple-product; and second, the two inequivalent dimers per unit cell give rise to the “flavor” index $i = 1, 2$ which in fact transforms

like a *spatial* vector index under discrete lattice point group operations, allowing a linear gradient to complete a point-group scalar. Note that even the sub-model defined in the next section, obtained by forgetting *e.g* the order parameters on the horizontal bonds, contains such a cubic term : the presence of the two complex vector fields $\vec{\phi}_1$ and $\vec{\phi}_2$ only enlarges the number of independent cubic terms, but does not change the essential features. We will see that these cubic terms *qualitatively* modify the properties of these field theories. Since such terms are non-vanishing *only* for field configurations in which the fluctuating magnetization has multiple orthogonal components, this indicates that *non-collinear* magnetic order plays a significant role in the physics.

B. Sub-Model

Even in 3D, and certainly in 2D, the non-quadratic terms in the effective action are crucial in determining the nature of the ordered phase which occurs for $r < 0$. To get a feeling for the effects of the cubic and quartic interactions, it is helpful to consider a deformation of the GSS model obtained by increasing the exchange constant along the solid vertical bonds, leaving the solid horizontal bonds unchanged. This splits the degeneracy of the two branches of triplet excitations, and has the effect in the field theory of adding an additional $\delta J \vec{\phi}_2^* \cdot \vec{\phi}_2$ term to $S^{(2)}$, thereby creating an effective quadratic Landau coefficient $r_2 = r + \delta J > r$ for the $\vec{\phi}_2$ field. Thus when $r \rightarrow 0$, the coefficient r_2 remains positive, and the still massive $\vec{\phi}_2$ field can be integrated out in the critical region. One is left with a “sub-model” involving only terms (with slightly renormalized coefficients) in Eqs. 8 depending only on the field $\vec{\phi}_1$:

$$S_{\text{sm}} = \int_{\mathbf{x}\tau} \left\{ \vec{\phi}_1^* (Z\partial_\tau + R - C\nabla^2)\vec{\phi}_1 - iG\partial_x(\vec{\phi}_1 + \vec{\phi}_1^*) \cdot \vec{\phi}_1 \times \vec{\phi}_1^* + U(\vec{\phi}_1 \cdot \vec{\phi}_1^*)^2 + V(\vec{\phi}_1 \cdot \vec{\phi}_1)(\vec{\phi}_1^* \cdot \vec{\phi}_1^*) + W[(\vec{\phi}_1 \cdot \vec{\phi}_1)(\vec{\phi}_1 \cdot \vec{\phi}_1^*) + \text{c.c.}] \right\}, \quad (9)$$

where we have, without loss of generality, rescaled the spatial axes to make the kinetic term (with coefficient C) isotropic (note that this is not possible in the full model). From the point of view of symmetries, this ‘sub-model’ can be defined as the DFT invariant under the above defined time reversal symmetry, reflection with respect to x and y (the latter having a trivial effect on the field : $\phi \rightarrow \phi$), and for which the boson vacuum is an exact eigenstate. The mean-field theory of Eq. 9 is solved exactly in Sec. III A 1.

III. LANDAU THEORY AND MEAN-FIELD PHASE DIAGRAM

Remarkably, simple power counting (see Sec. V) indicates that *both* the cubic and quartic terms (in $S^{(3)}$ and $S^{(4)}$ respectively) are *marginal* in the Renormalization Group (RG) sense in two spatial dimensions (2D), which plays the role of the upper critical dimension in critical phenomena. In three dimensions, the cubic and quartic interactions are *irrelevant* at the critical point, affording the possibility of an unusual mean-field critical point in a three-dimensional (3D) system. In this section, we study this mean-field behaviour in details. For pedagogical rea-

sons, we will not consider the MFT of the full model (8) as the physics of the solutions may be obscured by the intrinsic complexity of this field theory. Instead, we will focus on the above-defined sub-model whose mean-field analysis will capture the essential physics of the full MFT phase space. This analysis, carried in the next section, establishes the existence of three phases : a phase where spins are antiparallel on each dimer, a chiral phase in which there is no static local magnetization, but the two spins maintain a fixed normal relative orientation while “rotating” quantum-mechanically with respect with each other on the dimer, and a spiral phase. The discussion of the antiferromagnetic “Néel” phase of the GSS model, which corresponds to a Mott insulator in terms of the lattice bosons, is postponed to the next section.

A. Sub-Model

1. Mean-Field solutions

Within the sub-model, consider first $G = 0$, in which the action becomes rotationally-invariant (under spatial rotations). If, furthermore, $V = W = 0$, Eq. 9 has an $O(6)$ symmetry under global orthogonal rotations of the six-component vector composed of the real and imaginary parts of $\vec{\phi}$. Thus, for $V = W = 0$, in mean-field theory (MFT), the system undergoes a continuous $O(6)$ symmetry-breaking transition as $R \rightarrow 0$ to a state with an arbitrary complex expectation value $\langle \vec{\phi} \rangle \neq 0$, and $\langle \vec{\phi} \rangle^* \cdot \langle \vec{\phi} \rangle = -R/2U$ for $R < 0$. The V and W terms re-

duce the $O(6)$ symmetry down to $O(3) \times U(1)$ and $O(3)$, respectively. For $V > 0$, it is helpful to decompose $\vec{\phi}$ into real and imaginary parts: $\vec{\phi} = \vec{\eta} + i\vec{\xi}$, where $\vec{\eta}$ and $\vec{\xi}$ are real vectors. For $W = 0$ and $V > 0$, the lowest energy states then have $|\vec{\eta}|^2 = |\vec{\xi}|^2$ and $\vec{\eta} \cdot \vec{\xi} = 0$, so that the order parameter becomes an orthogonal pair of fixed length vectors comprising a “frame”, similar to the order parameter in a bi-axial nematic liquid crystal. Including a non-zero W (with still $V > 0$) favors unequal (but still orthogonal) real and imaginary parts, and the MFT minima becomes instead $|\vec{\eta}| = |\vec{\phi}| \cos \psi$, $|\vec{\xi}| = |\vec{\phi}| \sin \psi$, with $\cos 2\psi = -W/V$. On the other hand, if $V < 0$ and $W = 0$, the MFT ground state is of the form $\langle \vec{\phi} \rangle = |\vec{\phi}| \hat{n} e^{i\alpha}$, with an arbitrary real unit vector \hat{n} and phase α , corresponding to parallel real and imaginary components. Including non-zero W simply breaks the phase degeneracy to favor $e^{i\alpha} = 1, i$ for $W < 0$ and $W > 0$, respectively.

Now consider including $G \neq 0$. It is instructive to rewrite the cubic term as $-iG\partial_x(\vec{\phi} + \vec{\phi}^*) \cdot \vec{\phi} \times \vec{\phi}^* = 4G\partial_x\vec{\eta} \cdot \vec{\eta} \times \vec{\xi}$. By inspection, a non-zero G thus favors *spatially non-uniform* configurations in which $\vec{\eta}$ precesses around $\vec{\xi}$ as one proceeds along the x axis. Physically (see below), this precession corresponds to spiral magnetic order. We allow for this by considering x -dependent configurations. Defining polar and azimuthal angles, θ and φ respectively, of $\vec{\eta}$ in the spherical coordinates defined with $\vec{\xi}$ along the polar axis, this term is written $-4G|\vec{\phi}|^3 \cos^2 \psi \sin \psi \sin^2 \theta \partial_x \varphi$. For fixed, constant $|\vec{\phi}|$ and θ , the mean-field Lagrange density becomes then

$$\mathcal{L}_{\text{sm}}^{\text{MF}} = C|\vec{\phi}|^2 \cos^2 \psi \sin^2 \theta (\partial_x \varphi)^2 - 4G|\vec{\phi}|^3 \cos^2 \psi \sin \psi \sin^2 \theta \partial_x \varphi + |\vec{\phi}|^4 \left\{ U + V [\cos^2 2\psi + \sin^2 2\psi \cos^2 \theta] + 2W \cos 2\psi \right\}. \quad (10)$$

The optimal precession wavevector is thus $Q = \partial_x \varphi = 2(G/C)|\vec{\phi}| \sin \psi / \sin \theta$ (the singularity as $\theta \rightarrow 0$ does not influence the results). Using this frequency, the Lagrange density becomes

$$\mathcal{L}_{\text{sm}}^{\text{MF}} = |\vec{\phi}|^4 \left\{ -(G^2/C) \sin^2 2\psi \sin^2 \theta + U + V [\cos^2 2\psi + \sin^2 2\psi \cos^2 \theta] + 2W \cos 2\psi \right\}. \quad (11)$$

Note that the contribution arising from minimization over Q is of the same order ($O(|\vec{\phi}|^4)$) as the U and V interactions, which is the MFT manifestation of G being marginal at the upper critical dimension. The minimum

energy (action) configurations are then found to be

$$\begin{aligned} (i) \quad & \theta = \pi/2, \quad \cos 2\psi = -\frac{W}{V + G^2/C}, \\ & V + G^2/C > |W| > 0, \\ (ii) \quad & \theta = \pi/2, \psi = \frac{\pi}{2} \Theta(W) \quad |W| > V + G^2/C > 0, \\ (iii) \quad & \theta = 0, \psi = \frac{\pi}{2} \Theta(W) \quad V + G^2/C < 0, \end{aligned} \quad (12)$$

where $\Theta(W)$ is the Heavyside step function. In fact, the latter two solutions are physically equivalent, since when

$\psi = 0$ or $\psi = \pi/2$, $\vec{\phi}$ is either pure real or pure imaginary, and θ has no physical significance. Thus the precessing solutions occur only for $V + G^2/C > |W| > 0$. In this regime, however, a continuous transition occurs within mean-field theory (provided the stability condition $U > G^2/C + W^2/(V + G^2/C)$ holds) from the dimer to a spiral phase.

2. Phases

The physical meaning of these phases is best described by the three observables,

$$\vec{N}_{1\mathbf{x}} \equiv \vec{S}_a(\mathbf{x}) + \vec{S}_b(\mathbf{x}) = i\vec{b}_{1\mathbf{x}}^\dagger \times \vec{b}_{1\mathbf{x}}, \quad (13)$$

$$\Delta\vec{S}_{1\mathbf{x}} \equiv \vec{S}_a(\mathbf{x}) - \vec{S}_b(\mathbf{x}) = \vec{b}_{1\mathbf{x}} + \vec{b}_{1\mathbf{x}}^\dagger, \quad (14)$$

$$\vec{T}_1(\mathbf{x}) \equiv 2\vec{S}_a(\mathbf{x}) \times \vec{S}_b(\mathbf{x}) = -i(\vec{b}_{1\mathbf{x}} - \vec{b}_{1\mathbf{x}}^\dagger). \quad (15)$$

where \vec{T} stands for the chirality defined on each bond. The relation to the boson variables can be shown from Eqs. 4a-4b and the hard-core condition.

We expect that, using the above decomposition of $\vec{\phi}$ into real and imaginary parts, $\langle \Delta\vec{S}_1 \rangle = 2\text{Re}\langle \vec{\phi}_1 \rangle = 2\vec{\eta}$ and $\langle \vec{T}_1 \rangle = 2\vec{\xi}$. If both $\vec{\eta}$ and $\vec{\xi}$ are non-zero, then general principles require that $\langle \vec{N}_1 \rangle \neq 0$, and we expect $\langle \vec{N}_1 \rangle \propto \vec{\eta} \times \vec{\xi}$. The converse, however, does not follow: it is possible that $\langle \vec{S}_1^{\text{tot}} \rangle = \langle i\vec{b}_1^\dagger \times \vec{b}_1 \rangle \neq 0$ but $\langle \vec{b}_1 \rangle = 0$ (though this is not a mean-field state).

Armed with these relations, we can characterize the three different mean-field phases defined by (12) :

(i) for $V + G^2/C > |W| > 0$ have all three “order parameters” non-vanishing. Since $\vec{\xi}$ is constant in these solutions, the “chirality” \vec{T}_1 is fixed on each horizontal bond, as $\vec{\eta}$ precesses, both \vec{N}_1 and $\Delta\vec{S}_1$ spiral from bond to bond along the x direction. The non-spiral solutions are of two varieties. Thus in this *spiral* phase all three quantities are non-vanishing, with a fixed (i.e. spatially constant) chirality \vec{T}_1 on each horizontal bond. The spins themselves, however, spiral from bond to bond along the x direction, maintaining the condition $\langle \vec{N}_1 \rangle \cdot \langle \Delta\vec{S}_1 \rangle = 0$. In the special limit $G \rightarrow 0$, the *pitch* of this spiral vanishes, and the spiral phase goes over to a sort of biaxial spin nematic.

(ii) for $W > 0, V + G^2/C$, only $\vec{\xi} \neq 0$, and one has a *chiral* phase: $\vec{T}_1 \propto \vec{\xi} \neq 0$ but the spins themselves are disordered, i.e. $\langle \vec{S}_a \rangle = \langle \vec{S}_b \rangle = 0$.

(iii) for $W < 0, -|V + G^2/C|$, the chirality vanishes and the two spins on each bond are antiparallel, $\langle \vec{S}_a \rangle = -\langle \vec{S}_b \rangle \neq 0$. This *antiparallel* phase is thus characterized by a single non vanishing order parameter $\langle \Delta\vec{S}_1 \rangle \neq 0$,

In MFT, continuous phase transitions are possible between all pairs amongst the four (antiparallel, chiral, spiral, and dimer) phases except between the anti-parallel and chiral states, which is a first-order transition. A

schematic cut through the mean-field phase diagram for $R < 0$ is shown in Fig. 4.

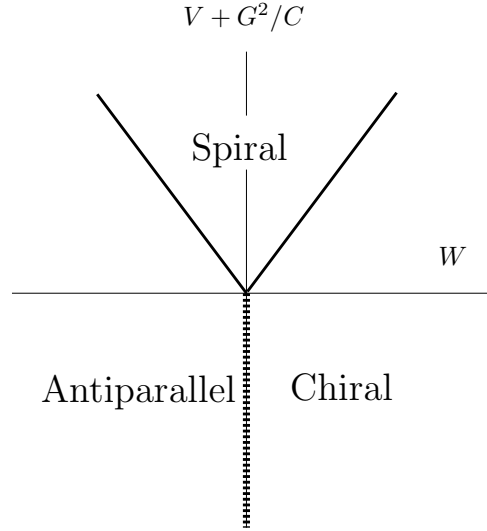


FIG. 4. Schematic cut through the mean-field phase diagram of the sub-model for $R < 0$.

Conspicuously absent from the MFT is a non-chiral ($\langle \vec{T}_1 \rangle = 0$) state with spontaneous magnetization on each dimer ($\langle \vec{N}_1 \rangle \neq 0$) but equal moment for each of the two dimer spins ($\langle \Delta\vec{S}_1 \rangle = 0$). As noted in the introduction, this is because such a state is *not* a triplet-boson condensate, $\langle \vec{b}_1 \rangle = 0$, i.e. not a “superfluid”. The absence of this “Néel” state is all the more troubling insofar as it is this state which corresponds to the antiferromagnetic state of the original SS model (with the vertical bonds removed by the additional interactions of the sub-model). As discussed in Sec. IV, such a “Néel” state is described in the bond-boson variables as a bosonic *Mott insulator*. Because such Mott insulators rely upon commensurability of the boson number with the lattice (i.e. in this case there is precisely one pair of aligned spins per horizontal bond), they are in fact outside the simple continuum description of Eqs. 8 or Eq. 9. A further consequence of the identification of the “Néel” state with the Mott insulator is that it cannot be obtained via a single continuous transition from the dimer phase (see below).

B. Full DFT

1. Mean-Field Phases

As emphasized above, the complexity of the full DFT renders an exhaustive analysis of even its mean-field phase diagram less than illuminating. However, the general sorts of phases which can arise are easily understood by analogy to the sub-model analysis above. In particular, with the two fields $\vec{\phi}_1$ and $\vec{\phi}_2$, one expects “direct products” of the states obtained therein, i.e. with real,

imaginary, or non-collinear complex values independently for each field. Further, the quartic terms coupling both fields ($u_{2,3,4}$, $v_{2,3}$, and $w_{2,3,4}$) will select definite relative orientations and phases of these order parameters. Thus, even without the possibility of spatially-varying (i.e. spiral) solutions, the full DFT clearly sustains a panoply of unusual phases.

Much of this complexity, however, arises in regions of the phase diagram in which we are uninterested. For models not too much deformed from the original Shastry-Sutherland hamiltonian, we expect a strong tendency for ordered state to local antiferromagnetic magnetization. As shown above, such local order ($\vec{N}_1 = -\vec{N}_2 \neq 0$) requires non-collinear complex values for both $\vec{\phi}_1$ and $\vec{\phi}_2$, and moreover a specific orientation and relative phase to these two fields. It is straightforward to construct regions in the space of quartic couplings in which such states are favored¹⁶ (although the task of computing the full such region is formidable!). Indeed, an effective Lagrangian in this subspace is naturally obtained by a direct rewriting of the Shastry-Sutherland spin Hamiltonian using Eqs. (4) and very naive coarse-graining of the quartic interactions.¹⁶ Thus, in the absence of cubic terms, the DFT could naturally describe transitions from the dimer state to a state with Néel order, at least at the mean-field level. As we show below, however, the non-vanishing cubic terms modify this conclusion significantly.

2. Spiral instability of Néel order

As noted above, a striking feature of the mean-field phase diagram for the sub-model (Fig. 4) is the absence of a phase with commensurate Néel order, i.e. with $\langle \vec{S}_{1\mathbf{x}}^{\text{tot}} \rangle = \vec{N}$ equal to a constant. Instead, the only phase with a net average on each bond moment is the spiral state, in which the spin density wave order shifts to a small non-zero wavevector and precesses in spin space. Uniform Néel ordering occurs only in the limiting case in which the quantum critical points to the dimer or anti-parallel states are approached.

In this subsection, we show that this behavior continues to hold in the full set of GSS models. More precisely, without fine tuning of parameters, in any *dimer bose condensate with a non-zero local Néel order*, this Néel vector forms an incommensurate spiral with a long pitch.

We consider a Néel phase corresponding to uniform expectations values $\langle \vec{\phi}_1 \rangle = A\hat{e}_1 + iB\hat{e}_2$ and $\langle \vec{\phi}_2 \rangle = \langle \vec{\phi}_1^* \rangle = A\hat{e}_1 - iB\hat{e}_2$ where \hat{e}_1 and \hat{e}_2 are two orthogonal vectors. This state is characterised as needed by antiferromagnetic order $\langle \vec{N}_1 \rangle = i\langle \vec{\phi}_1^* \times \vec{\phi}_1 \rangle = -\langle \vec{N}_2 \rangle = i\langle \vec{\phi}_2^* \times \vec{\phi}_2 \rangle = -2AB\hat{e}_3$ where $\hat{e}_3 = \hat{e}_1 \times \hat{e}_2$. Moreover, on each bond the chirality is given by $\vec{T}_1 = 2B\hat{e}_2 = -\vec{T}_2$, and $\Delta\vec{S}_1 = \Delta\vec{S}_2 = 2A\hat{e}_1$.

To study the stability of this Néel phase with respect to spiral order, we consider spatial-dependant small rotations of the normalized triad $\hat{e}_1, \hat{e}_2, \hat{e}_3$ defined above.

The rotations with respect to these three axis are respectively parametrized by the three angles $\theta_1, \theta_2, \theta_3$. The usual gradient contribution to the energy of these fluctuations, \mathcal{L}_θ^0 , from the quadratic part $S^{(2)}$ of the action (8a) is :

$$\mathcal{L}_\theta^0 = c_1 [B^2(\partial_x\theta_1)^2 + A^2(\partial_x\theta_3)^2 + (A^2 + B^2)(\partial_x\theta_3)^2] + (x \rightarrow y, c_1 \rightarrow c_2). \quad (16)$$

Next consider the effect of the cubic terms which depend explicitly on the spatial variations of $\vec{\phi}_1, \vec{\phi}_2$ and are thus directly sensitive to these chiral instabilities. Note that $\vec{\phi}_1 = \vec{\phi}_2^*$ (needed to make $\vec{N}_1 = -\vec{N}_2$), and moreover the fluctuations considered leave this equality unchanged. Hence the g_2 and g_4 terms in (8b) do not contribute to the energy of these local rotations. From the two others, we get a quadratic contribution,

$$\mathcal{L}_\theta^1 = 4(g_0 - g_1)A^2B \theta_1(\partial_x\theta_3 - \partial_y\theta_3). \quad (17)$$

The resulting action for the θ fluctuations is obviously not definite positive, except with the special fine tuning $g_0 = g_1$ or $A = 0$ or $B = 0$. This completes the proof of the above assertion that the “Néel” phase is unstable to a weak spiral deformation, as a non-vanishing texture in θ will always develop for some momentum \mathbf{Q} . Although this proof was made specifically within the DFT theory, the conclusion is in fact more general and rests only upon the symmetries of the GSS models. Briefly, the massless of all three of the θ modes is required by Goldstone’s theorem, since there are no unbroken subgroups of the SU(2) spin-rotation symmetry. Similarly, linear gradient terms of the form in Eq. (17) are generically present by symmetry, since $\Delta\vec{S}_{1\mathbf{x}} = \Delta\vec{S}_{2\mathbf{x}} \propto \hat{e}_1$ breaks reflection invariance. Thus the dimer bose condensate does not generically describe a state with uniform Néel order.

IV. BOSONIC MOTT INSULATORS

A. Sub-model

As discussed in the introduction, it is clear from Eqs. 13-15 that a state with spontaneous collinear and aligned moments on the two sites of each bond of the SS lattice cannot be described as a dimer-boson condensate. Instead, these are Mott insulators. To understand the physics of such states, we first discuss the simple example of the “antiferromagnetic” state in the bond-boson field theory for the sub-model. The only known non-superfluid ground states of interacting boson systems without disorder are bose solids or Mott insulators, the latter being most simply understood as a bose solid pinned by a commensurate lattice potential. Because the desired state does not break translational symmetry, we are led to consider a bosonic Mott insulator as a candidate state. To do so, we are required to include the effects of the underlying lattice. A “microscopic” means of including these lattice

effects would be to return to the description in terms of the $\vec{b}_{1\mathbf{x}}, \vec{b}_{1\mathbf{x}}^\dagger$ operators. Instead, we continue to employ an *effective* field theory approach, both for consistency with the remainder of the paper and on the grounds that direct analytic treatments of the microscopic model have no control parameter and are hence unreliable. On symmetry grounds, lattice effects can be included by addition additional terms to the effective action which break the continuous Galilean invariance of S_{sm} down to the discrete space-group symmetries of the lattice. This is accomplished by including a *periodic potential* for the bosons:

$$S_{\text{sm}} \rightarrow \tilde{S}_{\text{rm}} \equiv S_{\text{sm}} + S_{\text{sm}}^{\text{lattice}}, \quad (18)$$

where

$$S_{\text{sm}}^{\text{lattice}} = \int_{\mathbf{x}\Gamma} \mathcal{U}(\mathbf{x}) \vec{\phi}^* \cdot \vec{\phi}, \quad (19)$$

where $\mathcal{U}(\mathbf{x})$ is an arbitrary periodic function with the symmetries of the GSS lattice, i.e. $\mathcal{U}(\mathbf{x} + \mathbf{a}_1) = \mathcal{U}(\mathbf{x} + \mathbf{a}_2) = \mathcal{U}(\mathbf{x})$. If desired, $\mathcal{U}(\mathbf{x})$ could be specified by its Fourier coefficients at reciprocal lattice vectors. We will not, however, require a specific form for the heuristic considerations of this section.

For the modified action \tilde{S}_{sm} , a simple analysis strongly suggests that the ‘‘Néel’’ state should occur if V is large and positive. To see this, it is useful to rewrite

$$\begin{aligned} U(\vec{\phi} \cdot \vec{\phi}^*)^2 + V(\vec{\phi} \cdot \vec{\phi})(\vec{\phi}^* \cdot \vec{\phi}^*) \\ = (U + V)(\vec{\phi} \cdot \vec{\phi}^*)^2 - V(i\vec{\phi}^* \times \vec{\phi})^2. \end{aligned} \quad (20)$$

Thus, positive V indeed favors configurations with $\vec{S}_1^{\text{tot}} \propto i\vec{\phi} \times \vec{\phi}^* \neq 0$. The last term in Eq. 20 can be decoupled using a Hubbard-Stratonovich transformation,

$$-V(i\vec{\phi}^* \times \vec{\phi})^2 \rightarrow -\vec{N} \cdot i\vec{\phi}^* \times \vec{\phi} + N^2/4V. \quad (21)$$

We may envision a treatment in which the ‘‘order parameter’’ \vec{N} is taken account in the saddle-point approximation, but the bosons themselves are treated exactly. The task then would be to find the ground state for the $\vec{\phi}$ bosons in the presence of an arbitrary (presumed constant for simplicity) \vec{N} , and subsequently to determine the optimal \vec{N} by energy minimization. At the single-particle level, \vec{N} appears essentially as a ‘‘Zeeman field’’ splitting the triplet of bosons into three inequivalent states. In the absence of the periodic potential, these have single-particle energies

$$\epsilon_m(\mathbf{k}) = R + Ck^2 - |\vec{N}|m, \quad (22)$$

where $m = -1, 0, 1$ is the angular momentum projection of the boson along the \hat{N} axis (e.g. for $\vec{N} = |\vec{N}|\hat{z}$, the three boson eigenstates are $\phi_\pm = (\phi_x \pm i\phi_y)/\sqrt{2}$, $\phi_0 = \phi_z$). Thus with $|\vec{N}| \neq 0$, the $m = 1$ state has lowest energy. For $|\vec{N}| > R$, the ground state necessarily

contains these bosons. If $|\vec{N}|$ is large, it is reasonable to ignore the $m = 0, -1$ bosons which have larger energy and need not be present.

In the absence of the periodic potential there is no alternative but for these $m = 1$ bosons to condense, giving rise to a state with either \vec{T} or $\Delta\vec{S}$ (or both) non-zero. In the full effective action, \tilde{S}_{sm} , however, another possibility exists. Indeed, assuming $\phi_0 = \phi_{-1} = 0$, \tilde{S}_{sm} describes a system of short-range *interacting* bosons in a periodic potential. If the density of these bosons is sufficiently large (i.e. the boson ‘‘chemical potential’’ $R - |\vec{N}|$ is sufficiently negative), and $\mathcal{U}(\mathbf{x})$ is strong, it may be energetically favorable for one boson to ‘‘localize’’ in each minima of $\mathcal{U}(\mathbf{x})$, more bosons being prevented from localizing by the short-range repulsion U . This is the desired bosonic Mott insulator, which has the properties of the antiferromagnet, to wit, an expectation value of the total spin on each dimer, without coincident ‘‘Bose condensation’’, i.e. $\langle \vec{T} \rangle = \langle \Delta\vec{S} \rangle = 0$. Clearly, the antiferromagnetic state requires *large* $|\vec{N}|$, and hence cannot be accessed by a continuous transition from the dimer phase.

B. WISDW to AF transition

Armed with the physical picture described above for the sub-model, we now turn to a long-wavelength description of the analogous Mott-insulating physics in the full GSS Hamiltonian. In particular, we focus on the question of the nature and order of a hypothetical transition between the AF and WISDW states. Because both phases sustain Néel order, it is valid to assume from the onset an expectation value \vec{N} of the order parameter. For simplicity, we will neglect (quantum) fluctuations of \vec{N} . By doing so, we ignore the effects of the two antiferromagnetic magnon modes on the critical properties. We expect this to be a valid approximation for several reasons. First, both phases exhibit *long-range* spin-density-wave order, implying limited fluctuations of \vec{N} . Second, the linear dispersion, $\omega \sim v_s|k|$, of antiferromagnetic magnons implies that their characteristic frequencies are much higher than those of the critical modes, which scale approximately as $\omega \sim c|k|^2$. Thus, on the long time scales appropriate to the critical dynamics of the AF-WISDW transition, the magnons are expected to be irrelevant. An important caveat is that, in the ordered (WISDW) phase, because the magnetic wavevector becomes incommensurate, the magnon modes must become involved. We therefore expect that the coupling of magnons to the critical modes is *dangerously irrelevant*. The treatment of this section then suffices to understand the properties on the disordered (AF) side of the transition and in the critical regime, but not at very low ω, k on the ordered (WISDW) side.

The assumed constant \vec{N} couples to the Bose fields as

$$\mathcal{L}_{N-B} = -\vec{N} \cdot \left(i\vec{\phi}_1^* \times \vec{\phi}_1 - i\vec{\phi}_2^* \times \vec{\phi}_2 \right), \quad (23)$$

which, for $\vec{N} = |\vec{N}|\hat{z}$ can be rewritten in the angular-momentum basis as

$$\mathcal{L}_{N-B} = -|\vec{N}| \left(\phi_{1+}^* \phi_{1+} - \phi_{1-}^* \phi_{1-} - \phi_{2+}^* \phi_{2+} + \phi_{2-}^* \phi_{2-} \right), \quad (24)$$

with $\phi_{i\pm}$ defined as in the previous subsection. Near the AF-WISDW transition, the Néel order is well-developed, and a large splitting exists between the lowest energy ϕ_{1+} and ϕ_{2-} modes. It is therefore appropriate to integrate out the other four “massive” modes: $\phi_{10}, \phi_{1-}, \phi_{2+}, \phi_{20}$. The remaining two fields $\phi_+ = \phi_{1+}$ and $\phi_- = \phi_{2-}$ constitute the order parameters for the quantum phase transition.

To proceed, we develop a Landau theory for this critical point using the relevant symmetries. The symmetries that remain unbroken in the “disordered” (AF) phase are: (1) the U(1) spin rotational symmetry about the \hat{z} axis in spin space, (2) discrete spatial reflection symmetries in the x and y directions, (3) a combined spin-reflection (π rotation around the \hat{x} or \hat{y} spin axis) with a simultaneous $\pi/2$ spatial rotation, and (4) a combined $\pi/2$ spatial rotation and time-reversal operation.

Interestingly, the continuous U(1) spin-rotation symmetry acts as a simple phase rotation of the order parameters,

$$\phi_{\pm} \rightarrow e^{\pm i\theta} \phi_{\pm}, \quad (25)$$

where θ is an arbitrary U(1) phase. Note that although there are two complex order parameters, there is only a single U(1) invariance. The symmetries (3) and (4) respectively correspond to the transformation

$$\begin{pmatrix} x \\ y \end{pmatrix} \rightarrow \begin{pmatrix} y \\ -x \end{pmatrix}; \quad \begin{pmatrix} \phi_+ \\ \phi_- \end{pmatrix} \rightarrow \begin{pmatrix} \phi_- \\ -\phi_+ \end{pmatrix}, \quad (26)$$

and

$$\tau \rightarrow -\tau; \quad \begin{pmatrix} x \\ y \end{pmatrix} \rightarrow \begin{pmatrix} y \\ -x \end{pmatrix}; \quad \begin{pmatrix} \phi_+ \\ \phi_- \end{pmatrix} \rightarrow \begin{pmatrix} -\phi_-^* \\ \phi_+^* \end{pmatrix}. \quad (27)$$

Taking into account all the symmetries, the general Landau form of the effective Lagrange density, keeping constant terms and those leading order in time and spatial derivatives, is

$$\begin{aligned} \mathcal{L}_{AF-WISDW} = & \sum_{s=\pm} \phi_s^* [\partial_\tau - c(\partial_x^2 + \partial_y^2) + \tilde{r}] \phi_s \\ & + \delta c [\phi_+^* (\partial_x^2 - \partial_y^2) \phi_+ - \phi_-^* (\partial_x^2 - \partial_y^2) \phi_-] \\ & + d (\partial_x \phi_+ \partial_y \phi_- + \text{c.c.}) \\ & + \pi u (|\phi_+|^4 + |\phi_-|^4) + \pi v |\phi_+|^2 |\phi_-|^2 + \pi w (\phi_+^2 \phi_-^2 + \text{c.c.}), \end{aligned} \quad (28)$$

where \tilde{r} is proportional to the deviation from the (mean-field) AF-WISDW critical point. At the mean-field level, for $\tilde{r} > 0$, bond-boson order is absent, and the system is in the AF state, while for $\tilde{r} < 0$, the bond-bosons are condensed, and the system is a WISDW. Viewed as a field theory, the Lagrange density in Eq. (28), like that of the original DFT, describes complex Bose fields with dynamical critical exponent $z = 2$ at the Gaussian level. Power counting thus implies the upper critical dimension is again $d = 2$, so that in three dimensions, the AF-WISDW transition is mean-field-like and continuous. In two dimensions, such a transition may still occur, but fluctuation corrections may again be significant. Their effects are studied using the renormalization group in Sec. V A.

V. FLUCTUATION EFFECTS: RENORMALIZATION GROUP

We have seen that, at the mean-field level, the dimer-boson approach requires a minimum of two *continuous* quantum phase transitions to connect the dimer and AF states of a generic GSS model. Moreover, the explicit construction of Landau theories appropriate to these transitions demonstrates that the upper critical dimension for both critical points is $d = 2$. Thus for the marginal case of two dimensions fluctuation effects can be significant, and are fortunately amenable to study using the renormalization group (RG). In this section we perform RG analyses for both putative transitions. In both cases, because we are interested in the behavior precisely in the upper critical dimension, we do not expect to find a non-trivial fixed point (the analog of the Wilson-Fisher fixed point, should it exist, merges with the Gaussian one as $d \rightarrow 2$ from below). Rather, fluctuation effects can either leave the Gaussian fixed point stable, leading only to logarithmic corrections to mean-field critical behavior, or they may destabilize the Gaussian fixed point. In the latter case, the true behavior in the vicinity of the putative phase transition is more subtle, and requires argumentation beyond the simple RG.

Due to its relative simplicity, we reverse the order of the previous sections, and first discuss the AF-WISDW transition. In this case, we find that the Gaussian fixed point has a non-vanishing domain of stability. Thus the AF-WISDW critical point in $d = 2$ displays, up to logarithmic corrections, mean-field behavior: the correlation length $\xi \sim \tilde{r}^{-\nu}$ with $\nu = 1/2$, etc.. Next, we turn to the study of the transition between the Dimer phase and the WISDW, and more generally to the other mean-field like phase described in section III A 1. The conclusion of exceptionally involved calculations is in stark contrast to that for the AF-WISDW transition. Regardless of the “bare” values of the coupling constants, without excessive fine-tuning, fluctuations always drive the system away from the Gaussian fixed point. Thus mean-field

behavior definitely does not apply in the naive critical regime, and moreover a more complex critical scenario may obtain. We argue that a natural possibility is that fluctuations nucleate an intermediate phase between the dimer and WISDW states. This intermediate phase is very likely to be an exotic, “fractionalized” state without long-range magnetic order but with elementary excitations carrying spin-1/2, as suggested recently by a completely different large- N approach.¹⁷

A. RG for the AF–WISDW transition

The AF-WISDW transition is described by the Lagrange density in Eq. 28. To determine the modifications to mean-field behavior, it is sufficient to carry out an RG analysis to one-loop in the quartic interactions u , v , and w . The classical RG techniques needed to derive the equations can be found in numerous textbooks¹⁸. A convenient way to proceed is the so-called floating cut-off procedure. For simplicity, we will consider in this discussion a hard cut-off, where the fields ϕ_{\pm} are defined for momenta $0 < |\mathbf{q}| < \Lambda$, although in the following we will switch to other regularizations. Let us consider the partition function $Z = \int d[\phi_{\pm}] d[\phi_{\pm}^*] e^{-S(\phi_{\pm}, \phi_{\pm}^*)}$. Under a change of cut-off $\Lambda \rightarrow \Lambda' = \Lambda/b$, we can split the measure of integration $d[\phi_{\pm}]$ into an integration over ‘fast modes’ $\phi_{\pm}^>$ and ‘slow modes’ $\phi_{\pm}^<$, where $\phi_{\pm}^>(\mathbf{q})$ is non zero only for $\Lambda/b < |\mathbf{q}| < \Lambda$, and $\phi_{\pm}^<(\mathbf{q})$ for $|\mathbf{q}| < \Lambda' = \Lambda/b$. The averaging over the ‘fast modes’ defines the remaining interactions between the slow modes with *renormalized* couplings, once we have rescaled the fields and momenta according to

$$\phi_i^< \rightarrow b^{\zeta} \phi_i' ; \quad x \rightarrow bx' ; \quad t \rightarrow b^z t'. \quad (29)$$

The fast mode integration is performed using the cumulant expansion, which to second order reads

$$\delta S = \langle S_I \rangle - \frac{1}{2!} \langle S_I^2 \rangle_c, \quad (30)$$

where S_I is the non-quadratic part of the action in Eq. 28, and $\langle \rangle_c$ corresponds to the connected averaged over the ‘fast modes’ using the weight defined by the quadratic Lagrangian (i.e. setting $u = v = w = 0$). We do this for infinitesimal rescaling $b = e^{dl}$, where $dl \rightarrow 0^+$ is a positive infinitesimal, and l is the cumulative (logarithmic) rescaling.

The freedom of choosing ζ and z during rescaling in Eqs. 29 is sufficient to keep the *isotropic* part of the quadratic Lagrangian fixed as the fast modes are integrated out, and we choose this convention. The Lagrangian has, however, two additional parameters, δc and d , which parameterize deviations from spatial isotropy (rotational invariance). With some effort, the one-loop RG for the quartic interactions can be done to *all orders* in δc and d , since these couplings are quadratic in the fields. However, the freedom to rescale under the RG

is insufficient to maintain scale-independent values of δc and d at the fixed point, so these couplings will themselves obey flow equations. From prior experience, we expect δc and d to in fact renormalize to zero, so that ultimately they may also be treated perturbatively.

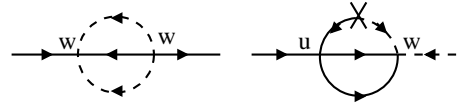


FIG. 5. Leading-order two-loop contributions to δc and d .

To verify this, we consider the leading-order renormalization of δc and d . This occurs first at *two loop* order, by the diagrams in Fig. 5. Taking into account their effects on both the isotropic terms and δc and d , we obtain the flow equations

$$\partial_l(\delta c) = -\frac{4}{27}w^2(\delta c), \quad (31a)$$

$$\partial_l d = -\frac{1}{9} \left[w^2 + \frac{1}{8}uw \right] d. \quad (31b)$$

Hence for δc always flows to zero, as does d in the non-vanishing basin of attraction $uw > -8w^2$. Thus the isotropic point is locally (marginally) stable and we can restrict our study to an isotropic propagator with $\delta c = d = 0$.

The one-loop RG equations for the quartic coupling constants are then readily obtained and read

$$\partial_l u = -u^2 - w^2, \quad (32a)$$

$$\partial_l v = -v^2 - 4w^2, \quad (32b)$$

$$\partial_l w = -(u + v)w. \quad (32c)$$

Hence, while u and v always renormalize downwards to negative values, w can either decrease to zero or diverge depending on the sign of $u + v$. A schematic RG flow of the above equations (32) is shown on figure 6.

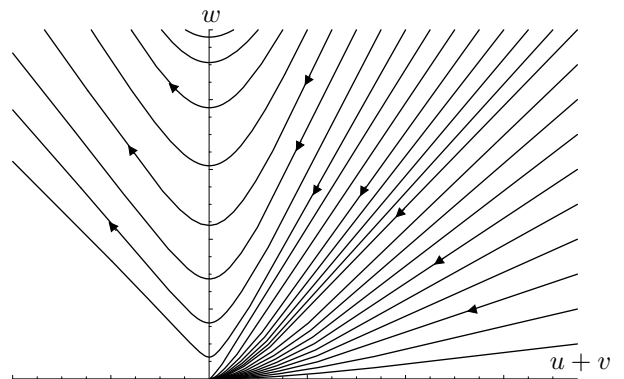


FIG. 6. RG flow for $v_0 = .1$, $w_0 = .1$ and $-0.1 < u_0 < 0.65$. The flow is shown in coordinates $u + v, w$.

As seen in the figure, there is a finite region of bare values for u, v, w for which the RG flows lead back to the Gaussian fixed point. Analytically, one can show that asymptotically stable solutions exist for which $u + v \simeq 2/l$, $u - v \simeq u_0/l^2$, and $w \simeq w_0/l^2$, where u_0 and w_0 are constants. The separatrix surface between the two phases, shown on the figure, can be shown to correspond to the asymptotic behaviour around the origin : $u + v \simeq l^{-1}[1 + \frac{1}{2}(\ln l)^{-1} + \mathcal{O}(\ln^{-2} l)]$, $u - v \simeq l^{-1}[1 - \frac{5}{6}(\ln l)^{-1} + \mathcal{O}(\ln^{-2} l)]$, $w \simeq \pm l^{-1}[\frac{1}{\sqrt{6}}(\ln l)^{-1} + \mathcal{O}(\ln^{-2} l)]$.

The renormalization study thus confirms the existence of a continuous transition between the AF and WISDW phases, which is, up to logarithmic corrections, of the mean-field type. As remarked above, we expect the antiferromagnetic magnons to be (dangerously) irrelevant at the critical point we found, but this expectation remains to be confirmed by detailed calculations beyond the scope of this paper.

B. RG for the dimer–WISDW transition

We now turn to the effect of quantum fluctuations on the dimer-WISDW transition, described by the action (8). This requires extending the RG analysis of the previous subsection to the much more formidable Lagrangian for the DFT. The crucial and new feature of the DFT (8) relative to the reduced Lagrangian for the AF-WISDW transition, is obviously the cubic terms (8b) which are directly related to the geometry of the SS lattice and the exactness of the SS dimer state. Much of the technical difficulties of the RG approach can be related to the presence of this term, which as we saw in the previous sections, will favor spatially non-uniform and non-collinear fluctuations.

On the technical side, the huge number of coupling constants in the action (8) can be conveniently handled using tensorial notation. These notations, the technical details of our approach, and the explicit RG equations are postponed to the appendix A. We here focus on the spirit of the method and the structure of the results. These are used to numerically study the scaling behaviour of the action (8) perturbatively in the couplings of the cubic and quartic terms. We find that these interaction coefficients always grow in magnitude under the RG, indicating a be-

haviour different from the mean-field one. The technical aspects of these calculations are somewhat formidable, and the less strong-willed reader may wish to skip at this point to the end of this subsection, where we discuss the *results and consequences* of the RG calculations. Others should press on for a brief summary of the calculations, and true aficionados, if any there be, will find further details in appendix A.

1. Idea of the method

As for the AF-WISDW transition, we simplify the calculations by working perturbatively in the violations of anisotropy δc and d . In this way, one may derive one-loop RG equations for the tensorial couplings G, U, V, W . These are represented graphically in Fig. 7.

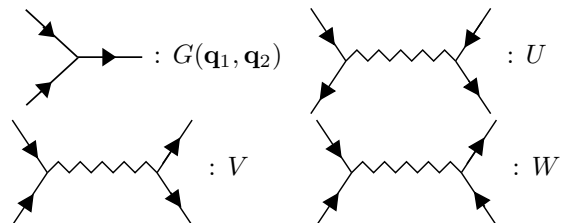


FIG. 7. Diagrammatic representation of terms in $S^{(3)}$ and $S^{(4)}$. Ingoing arrows correspond to *e.g.* $\vec{\phi}^*$. Complex conjugates of the above diagrams have been omitted for clarity.

The specificity of the field theory (8) is obviously the cubic term (8b). It induces most of the differences between our results and the more conventional renormalization of a $\vec{\phi}^4$ field theory. As the first of its consequences, we must consider up to the fourth term in the cumulant expansion that defines the renormalised action :

$$\delta S = \langle S_I \rangle > - \frac{1}{2!} \langle S_I^2 \rangle_c > + \frac{1}{3!} \langle S_I^3 \rangle_c > - \frac{1}{4!} \langle S_I^4 \rangle_c >, \quad (33)$$

where $S_I = S^{(3)} + S^{(4)}$. In each of these terms, only one-loop diagrams are considered. The result can be organized by collecting the contribution to the renormalized propagator and G, U, V, W (shown as black boxes on figure 8). The different 1-loop diagrams are shown in figure 8.

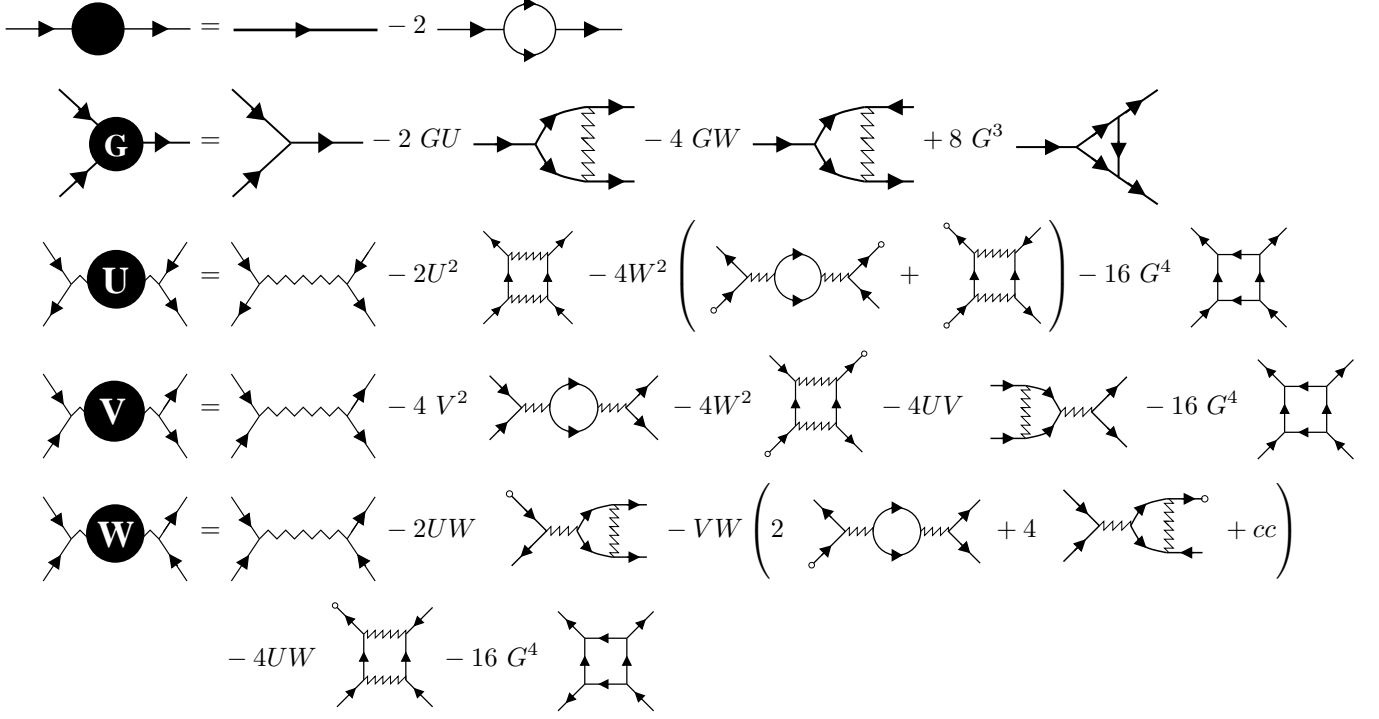


FIG. 8. Diagrammatic representation of the contributions of order one loop to the renormalised coupling tensors G, U, V, W and the propagator C .

One can notice that the peculiar cubic term ' G ' gives rise to contributions both to the anomalous dimensions and *all* the coupling constants. In particular, it renormalizes itself to order G^3 and the quartic couplings to order G^4 . The unusual derivative nature of these interactions requires consideration of non-trivial vertices at non-vanishing external momentum even in the one-loop RG, which is extremely unusual.

Due to their complexity, the different contributions are presented in the appendix A. We here focus on the structure of the RG equations. From the result of appendix A, we find the value of ζ and the dynamical exponent z to order one loop :

$$\zeta = -1 - \frac{1}{8\pi} (g_0^2 + g_2^2) - \frac{1}{16\pi} (g_1 + g_4)^2 \quad (34)$$

$$+ \frac{1}{16\pi} [\delta c(g_0^2 - g_2^2) + d(g_0 + g_2)(g_1 + g_4)],$$

$$z = 2 + \frac{1}{8\pi} (g_0^2 + g_2^2 + g_1^2 + g_4^2) \quad (35)$$

$$- \frac{1}{16\pi} \left[\frac{1}{2} \delta c(g_0^2 - g_2^2 + g_4^2 - g_1^2) + d(g_0 g_4 + g_1 g_2) \right].$$

As shown in the appendix, using these exponents and the direct contributions of the diagram to the couplings G, U, V, W , we obtain the non-linear RG equations describing the scaling behaviour of the couplings of the field

theory (8). For simplicity, we present here only the structure of these equations. The brave and bold reader who might be interested in the detailed definition of the tensorial coefficients of these equations can find the explicit equations at the end of the appendix.

The one-loop RG equations are

$$\partial_l g_i = -\frac{1}{32\pi} \Gamma_{jkl}^{(g,i)} g_j g_k g_l - \frac{1}{4\pi} \Theta_{jk}^{(i)} g_j u_k, \quad (36a)$$

$$\partial_l u_i = \left[-\frac{3}{8\pi} (g_0^2 + g_2^2) - \frac{1}{8\pi} (g_1 + g_4)^2 \right] u_i - \frac{1}{64\pi} \Gamma_{jklm}^{(u,i)} g_j g_k g_l g_m - \frac{1}{2\pi} \left(\Lambda_{jk}^{(1,i)} u_j u_k + \Lambda_{jk}^{(2,i)} w_j w_k \right), \quad (36b)$$

$$\partial_l v_i = \left[-\frac{3}{8\pi} (g_0^2 + g_2^2) - \frac{1}{8\pi} (g_1 + g_4)^2 \right] v_i - \frac{1}{2\pi} \left(\Lambda_{jk}^{(3,i)} u_j v_k + \Lambda_{jk}^{(4,i)} v_j v_k + \Lambda_{jk}^{(5,i)} w_j w_k \right) - \frac{1}{64\pi} \Gamma_{jklm}^{(v,i)} g_j g_k g_l g_m, \quad (36c)$$

$$\partial_l w_i = \left[-\frac{3}{8\pi} (g_0^2 + g_2^2) - \frac{1}{8\pi} (g_1 + g_4)^2 \right] w_i - \frac{1}{64\pi} \Gamma_{jklm}^{(w,i)} g_j g_k g_l g_m - \frac{1}{2\pi} \left(\Lambda_{jk}^{(6,i)} u_j w_k + \Lambda_{jk}^{(7,i)} v_j w_k \right). \quad (36d)$$

As expected, since $d = 2$ corresponds to the upper critical dimension of the DFT (8), the linear terms vanish in the right hand side of the above equations. All the perturbing operators of the free action thus correspond to either marginally relevant or marginally irrelevant perturbations. Due to the complexity of these non-linear flow equations, it is extremely difficult to determine the stability of the Gaussian fixed point analytically. Instead, we have concentrated on a numerical integration of Eqs. (36), supplemented with analytical treatment in particular limits. After a concerted effort to locate a stable basin of attraction, we have concluded that the ultimate fate of the RG, is a “run-away” flow in which several couplings tend to large (absolute) values as $l \rightarrow \infty$. We believe this to be true for generic bare parameters, i.e. for all initial conditions except for various special sets of parameters of measure zero in the space of marginal coupling constants.

The driving force for this instability is most easily illustrated for the simplified RG flows which apply to the sub-model, Eqs. A2 of appendix A. The most significant aspect of these equations is the RG flow for the cubic interaction,

$$\partial_l G = \frac{3}{16\pi} G^3, \quad (37)$$

which is *independent* of the other coupling constants. This equation immediately indicates the flow of G to large values, irrespective of its sign. As it does so, it tends to drive U and V negative, leading to their divergence as well: in fact, it can be shown from Eqs. A2 that U and V always diverge *before* G . Moreover, this instability is not generic in the absence of the cubic interaction: for $G = 0$ there is a finite basin of attraction for the Gaussian fixed point in the space of U, V, W .

Although the decoupling of the flow of the cubic interactions is not shared by the RG flows in the full DFT, the remaining properties of the sub-model RG are indeed common to the DFT. In particular, if all cubic interactions are *fine-tuned* to zero, there is a stable basin for the Gaussian fixed point. In a generic situation, however, with non-vanishing cubic terms, the flow is always to strong coupling. If the bare cubic couplings are taken initially small, the RG flows for the quartic interactions initially tend towards zero, but the cubic couplings slowly increase as this proceeds. Eventually, the feedback of the cubic terms into the RG for the quartic couplings drives one or more of these interactions into an obviously unstable regime, and the quartic interactions tend to large values. Like in the sub-model, it appears that the quartic couplings diverge before the cubic ones.

While strictly speaking such run-away RG flows indicate only the failure of the perturbative RG analysis, we can get some physical insight into the failure of the RG by considering the nature of the diverging RG. It is clear from the above discussion that the divergence is driven by the cubic coupling constants. Because each involves a triple product, such terms contribute to the action *only* for non-collinear configurations of the fields. Their role in the perturbative instability thus indicates that non-collinear magnetic correlations (or at least fluctuations) are significant in this critical regime. If the RG flows are followed out to the neighborhood of their actual divergence (this is justified for small bare couplings – see the discussion in Refs. 19,20), however, the quartic interactions become much larger than the cubic ones. Because the quartic terms do not involve spatial derivatives, this hints that the incipient ordering may in fact be *commensurate* (see, e.g. Sec. IIIC). Finally, the flow to negative quartic couplings suggests that the dominant field configurations (with largest effective action) have a non-zero amplitude in the putative critical regime.

Based on these arguments, it is natural to suspect that the behavior in this region of the phase diagram may be modeled a *Non-Linear σ Model* (NL σ M), in which the order-parameter amplitude is everywhere (and when) non-vanishing and hence approximated as fixed. The *orientation* of the order parameter may, however, fluctuate. To determine the appropriate NL σ M, we must specify the order parameter space. In order to incorporate the tendency towards antiferromagnetism favored by the J_2 spin-spin interaction, a natural choice is to consider configurations of $\vec{\phi}_{1,2}$ which sustain local Néel order. As explained in Sec. IIIC, such states have order parameters of the form

$$\vec{\phi}_1 = \vec{\phi}_2^* = A\hat{e}_1 + iB\hat{e}_2, \quad (38)$$

where in general A and B are fixed constants, while \hat{e}_1 and \hat{e}_2 are arbitrary *orthogonal* unit vectors, $\hat{e}_1 \cdot \hat{e}_2 = 0$, $\hat{e}_1^2 = \hat{e}_2^2 = 1$. The NL σ M space is defined by the set of all such orthogonal vectors, constraining the effective action by the spin-rotational and lattice invariances of

the GSS model. Closely related $NL\sigma$ Ms have been derived and studied previously for non-collinear magnets in Refs. 12. In addition to ordered phases, they are believed to sustain a magnetically disordered phase with *fractional* (i.e. spin-1/2) excitations, “spinons”. We thus guess that the flow of the RG to strong coupling may be indicative of such a fractionalized phase intervening between the WISDW and dimer states. Because the strong-coupling RG flow is, of course, not truly controlled, alternative scenarios are possible, including the less interesting possibility of a direct first-order transition between the latter two phases.

VI. SUMMARY

In this paper we have demonstrated the utility of the dimer-boson representation for quantum spin models. The approach enables a simple derivation of critical field theories, particularly suitable for systems with explicit dimerization. The coarse-grained dimer-boson order parameters describe a wide range of magnetic phases with complex local orders. In frustrated magnetic models such as the GSS models, this description gives a natural means to understand a diverse set of spin orderings that naturally obtain.

For the particular class of GSS models on which we have focused, the method indicates the absence of a direct dimer-AF quantum critical point, but leads to a two-stage transition through the intermediate WISDW phase. With three-dimensional coupling, the two transitions from this phase may be continuous and mean-field-like, while in strictly two dimensions quantum fluctuations destroy mean-field behavior near the putative dimer-WISDW critical point. We have argued on physical grounds that the likely alternative is the existence of a “fractionalized quantum paramagnet” between the dimer and WISDW states. We cannot rule out however other improbable scenarios. In particular, our 1-loop RG study was based on some technical assumption of ‘weakly anisotropic’ bosonic propagator which may be invalidated in some regimes.

More generally, the dimer-boson theory explored here has a very interesting field-theoretic structure, and may lead to a variety of potential extensions in the future. One might wish to derive a more precise complete MFT study of the full action (8). The dimer boson representation could likely be fruitfully applied to other frustrated magnetic models. We leave these and other extensions to future works.

Acknowledgements

Thanks to R. Singh for stimulating our interest in this problem so long ago, and to M. P. A. Fisher for discussions. This research was supported by the NSF CAREER program under Grant NSF-DMR-9985255, by the Sloan and Packard Foundations, and by National Science Foundation under Grant No. PHY99-07949.

APPENDIX A: EXPLICIT RG EQUATIONS

In this appendix, we present briefly the excruciating derivation of the scaling equations for the model (8) and the sub-model (9). The first step in the derivation of the RG equations is to determine all the necessary 1-loop terms in the cumulant expansion (33). This is conveniently achieved graphically using the conventions of Fig. 7, associated with the tensorial notations defined below. The result is shown in Fig. 8 as the definition of formal renormalized couplings and propagator (represented by black boxes). In these diagrams, each ‘internal line’ corresponds to a contraction between two ‘fast modes’, the external legs corresponding to the remaining slow modes.

The next step in this approach is to explicitly average over the internal fast modes for each of these diagrams. Special care has to be given here to the diagrams involving a cubic vertex (from Eq. (8b)) due to their explicit and anisotropic momentum dependence. The choice of the cut-off can then be of some importance. In principle, any universal feature (like ratios between the coefficients in the RG equations) is independent of the precise choice of *smooth* cut-off we choose. However in practice it is often useful to use a sharp cut-off, and one must be careful not to spoil the result by such a choice. The first and natural choice is a sharp isotropic cut-off function in momentum space: the fast modes then correspond to $\Lambda e^{-dt} < |\mathbf{q}| < \Lambda$. We then have to consider the dominant terms for large Λ in the integrals corresponding to the diagrams of fig. 8. Instead we will follow a more ‘field-theoretical’ route. We have checked term by term that these two methods give exactly the same result, which reinforces our confidence in the result.

In this approach, the regularized propagator $C_0^{-1}(\mathbf{q}, \omega)$ is expressed as

$$\int_{\Lambda^{-2}}^{+\infty} dt e^{-t(cq^2 + iZ\omega)}. \quad (\text{A1})$$

By differentiating the end result of each diagram with respect to $\partial/\partial \ln \Lambda$, we obtain the desired result.

Following this method, the contributions of the diagrams from Fig. 8 can be readily obtained for the sub-model Eq. (9) for which the meaning of the conventions (Fig. 7) is obvious. We will thus first present the results for this sub-model before turning back to the full DFT and the associated tensorial notations. For completeness, we will also describe in detail the contribution from the most specific diagram of Fig. 8 for the full DFT, and leave the generalization to the other diagrams for the motivated reader.

1. RG equations for the ‘‘sub-model’’

The anomalous dimension ζ of the field $\vec{\phi}$ and dynamical exponent read

$$\zeta = -1 - \frac{G^2}{8\pi} \quad ; \quad z = 2 + \frac{G^2}{8\pi}.$$

The scaling equations then follow :

$$\partial_l G = \frac{3}{16\pi} G^3, \quad (\text{A2a})$$

$$\partial_l U = -\frac{3}{8\pi} G^2 U - \frac{1}{2\pi} U^2 - \frac{5}{2\pi} W^2 - \frac{1}{8\pi} G^4, \quad (\text{A2b})$$

$$\partial_l V = -\frac{3}{8\pi} G^2 V - \frac{3}{2\pi} V^2 - \frac{1}{\pi} W^2 - \frac{1}{\pi} UV - \frac{1}{8\pi} G^4, \quad (\text{A2c})$$

$$\partial_l W = -\frac{3}{8\pi} G^2 W - \frac{3}{2\pi} (U + V)W + \frac{1}{4\pi} G^4. \quad (\text{A2d})$$

Note that these equations are a special case of the equations for the full DFT presented below, with the only non-zero couplings $G = -g_0, U = u_1, V = v_1, W = w_1$.

2. Tensorial notations for the full DFT

To closely follow the study of the sub-model and the corresponding 1-loop expansion of Fig. 8, we need to translate the definition of the full DFT into the tensorial coupling G, U, V, W , corresponding to the 4 couplings of the sub-model.

With this idea in mind, the quadratic part, Eq. (8a), of the action can be written as

$$S^{(2)} = - \int_{\mathbf{q}, \omega} \vec{\phi}_i^*(-\mathbf{q}, \omega) C(\mathbf{q}, \omega) \vec{\phi}_j(\mathbf{q}, \omega), \quad (\text{A3})$$

$$C(\mathbf{q}, \omega) = [C_0(\mathbf{q}, \omega) \delta_{ij} + D_{ij}(\mathbf{q})],$$

where $i = 1, 2$ or x, y , $C_0(\mathbf{q}, \omega) = (c q^2 + i Z \omega)$, $c = c_1 + c_2, \delta c = c_1 - c_2$ and

$$D_{ij}(\mathbf{q}) = \begin{pmatrix} \delta c (q_x^2 - q_y^2) & d q_x q_y \\ d q_x q_y & -\delta c (q_x^2 - q_y^2) \end{pmatrix}. \quad (\text{A4})$$

Similarly, the cubic term

$$S_{int}^{(3)} = \frac{i}{2} \int_{\mathbf{x}, \tau} \left\{ g_0 \vec{\phi}_1^* \cdot \left(\partial_x \vec{\phi}_1 \times \vec{\phi}_1 - \vec{\phi}_1 \times \partial_x \vec{\phi}_1 \right) \right. \\ + g_1 \vec{\phi}_2^* \cdot \left(\partial_x \vec{\phi}_1 \times \vec{\phi}_2 - \vec{\phi}_2 \times \partial_x \vec{\phi}_1 \right) \\ + g_2 \vec{\phi}_1^* \cdot \left(\partial_x \vec{\phi}_2 \times \vec{\phi}_2 - \vec{\phi}_2 \times \partial_x \vec{\phi}_2 \right) \\ \left. + g_4 \vec{\phi}_2^* \cdot \left(\partial_x \vec{\phi}_2 \times \vec{\phi}_1 - \vec{\phi}_1 \times \partial_x \vec{\phi}_2 \right) \right\} \quad (\text{A5})$$

can be rewritten as

$$S_{int}^{(3)} = -\frac{1}{2} \int_{\mathbf{q}_1, \mathbf{q}_2} \epsilon_{\mu\nu\rho} G_{ijk}(\mathbf{q}_1, \mathbf{q}_2) \\ \left[\vec{\phi}_{i,\mu}^*(\mathbf{q}_1 + \mathbf{q}_2) \vec{\phi}_{j,\nu}(\mathbf{q}_1) \vec{\phi}_{k,\rho}(\mathbf{q}_2) + \text{c.c.} \right], \quad (\text{A6})$$

where the coupling constant is given by

$$G_{ijk}(\mathbf{q}_1, \mathbf{q}_2) = \quad (\text{A7}) \\ g_0 \delta_{111} (q_{1x} - q_{2x}) + g_1 (\delta_{212} q_{1x} - \delta_{221} q_{2x}) \\ + g_2 \delta_{122} (q_{1x} - q_{2x}) + g_4 (\delta_{221} q_{1x} - \delta_{212} q_{2x}) \\ + (x \rightarrow y, 1 \leftrightarrow 2) \\ = \delta_{111} [g_0 (q_{1x} - q_{2x})] + \delta_{122} [g_2 (q_{1x} - q_{2x})] \\ + \delta_{212} [g_1 q_{1,x} - g_4 q_{2,x}] + \delta_{221} [g_4 q_{1,x} - g_1 q_{2,x}].$$

Here we have used the notation $\delta_{111} = \delta_{i,1} \delta_{j,1} \delta_{k,1}$, etc.. With similar notations, the quartic part (8c) reads

$$S^{(4)} = \int_{\mathbf{x}, \tau} \vec{\phi}_i^* \vec{\phi}_j^* (U^{ij;kl} + V^{ij;kl} + W^{ij;k,l}) \vec{\phi}_k \vec{\phi}_l, \quad (\text{A8})$$

with the coupling tensors

$$U^{ij;kl} = u_1 (\delta_{1111}^{ijkl} + \delta_{2222}^{ijkl}) + u_2 (\delta_{2211}^{ijkl} + \delta_{1122}^{ijkl}) \\ + u_3 (\delta_{2121}^{ijkl} + \delta_{1212}^{ijkl}) + u_4 (\delta_{2112}^{ijkl} + \delta_{1221}^{ijkl}), \quad (\text{A9a})$$

$$V^{ij;kl} = v_1 (\delta_{1111}^{ijkl} + \delta_{2222}^{ijkl}) + v_2 (\delta_{2211}^{ijkl} + \delta_{1122}^{ijkl}) \\ + v_3 (\delta_{2121}^{ijkl} + \delta_{1221}^{ijkl} + \delta_{1212}^{ijkl} + \delta_{2112}^{ijkl}), \quad (\text{A9b})$$

$$W^{ij;k,l} = w_1 (\delta_{1111}^{ijkl} + \delta_{2222}^{ijkl}) + w_2 (\delta_{2211}^{ijkl} + \delta_{1122}^{ijkl}) \\ + w_3 (\delta_{2121}^{ijkl} + \delta_{1221}^{ijkl} + \delta_{1212}^{ijkl} + \delta_{2112}^{ijkl}). \quad (\text{A9c})$$

3. Cubic diagram contribution

We choose to illustrate our method, and in particular our choice of regularization, on the contribution of G to order G^3 (see figure below). As the cubic term is a specificity of the DFT we developed in this paper, such a term is representative of the differences between the renormalization of this field theory with respect to conventional ones. The technical subtleties of the regularization will also appear clearer on this diagram than on any others, due to the explicit momentum dependence of the cubic term.

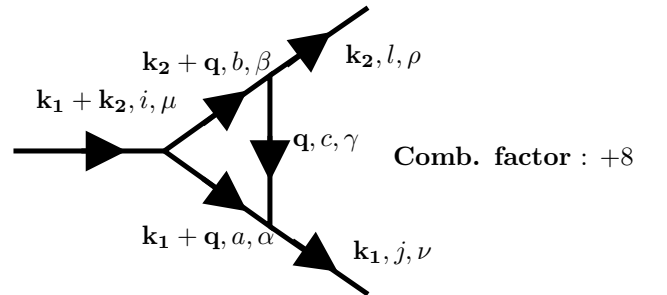


FIG. 9. Diagram corresponding to the renormalization of G to order G^3 .

With the momentum convention of Fig. 9, we can write the contribution of this G^3 diagram with the tensorial notations of the previous part as

$$\left(\frac{1}{2}\right)^3 \epsilon_{\mu\alpha\beta}\epsilon_{\beta\gamma\rho}\epsilon_{\nu\gamma\alpha} \quad (\text{A10})$$

$$\int_{\mathbf{q},\omega} C^{-1}(\mathbf{k}_1 - \mathbf{q}, \Omega_1 - \omega) C^{-1}(\mathbf{k}_2 + \mathbf{q}, \Omega_2 + \omega) C^{-1}(\mathbf{q}, \omega) \\ G_{iab}(\mathbf{k}_1 - \mathbf{q}, \mathbf{k}_2 + \mathbf{q}) G_{bcl}(\mathbf{q}, \mathbf{k}_2) G_{jca}(\mathbf{q}, \mathbf{k}_1 - \mathbf{q}).$$

The antisymmetric tensors $\epsilon_{\alpha\beta\gamma}$ come from the vector product in the definition of the cubic term (8b), and the factor $\frac{1}{2}$ is part of the convention we chose for the definition of the tensor G . In the above \mathbf{q} integral, the regularization (A1) is assumed for each of the three C^{-1} propagators. By explicitly integrating over ω we can get rid of one of the corresponding t integral (see (A1)) :

$$\int_{\omega} C^{-1}(\mathbf{k}_1 - \mathbf{q}, \Omega_1 - \omega) C^{-1}(\mathbf{k}_2 + \mathbf{q}, \Omega_2 + \omega) C^{-1}(\mathbf{q}, \omega) \\ = \int_{\Lambda^{-2}}^{+\infty} dt_1 \int_{\Lambda^{-2}}^{+\infty} dt_2 \exp\left[-2(t_1 + t_2)[\mathbf{q} + \mathbf{Q}]^2\right. \\ \left. - t_1(2\mathbf{Q}^2 + \mathbf{k}_1^2 + \mathbf{k}_2^2 + i(\Omega_1 + \Omega_2)) - t_2(2\mathbf{Q}^2 + \mathbf{k}_1^2 + i\Omega_1)\right],$$

with $\mathbf{Q} = \frac{1}{2}\left(\frac{t_1}{t_1+t_2}\mathbf{k}_2 - \mathbf{k}_1\right)$.

To lighten the writing, let us use the notations $X = 2Q^2 + k_1^2 + k_2^2 + i(\Omega_1 + \Omega_2)$ and $Y = 2Q^2 + k_1^2 + i\Omega_1$. These appear as factors respectively of t_1 and t_2 in the exponential in the result of the ω integration. After a change of variables, $\mathbf{q} \rightarrow \mathbf{q} + \mathbf{Q}$, the remaining \mathbf{q} dependant exponential becomes isotropic in \mathbf{q} . Hence, upon expanding the G^3 product in (A10), only two terms do not vanish by \mathbf{q} -reflection symmetry : the q_x^2, q_y^2 factor, and the constant factor. By power counting, it is easily realized that the former is the only one proportional to $\ln \Lambda$ in the limit $\Lambda \rightarrow \infty$.

Due to the change of variable, the q_x^2, q_y^2 term appear with two different t 's prefactors. The first prefactor corresponds to the integral

$$I_1 = \int_u^{+\infty} dt_1 \int_u^{+\infty} dt_2 \frac{t_1}{t_1 + t_2} \\ \int_{\mathbf{q}} q_x^2 e^{-2(t_1+t_2)q^2} (e^{-t_1 X} e^{-t_2 Y}). \quad (\text{A11})$$

The \mathbf{q} integral can then be performed explicitly, and we obtain the result

$$I_1 = \frac{1}{32\pi} \int_u^{+\infty} dt_1 \int_u^{+\infty} dt_2 \frac{t_1}{(t_1 + t_2)^3} (e^{-t_1 X} e^{-t_2 Y}).$$

We are interested in the leading term in the limit of large cut-off Λ which corresponds to

$$\partial_u I_1 = \frac{1}{32\pi} \frac{1}{u} \int_1^{\infty} dx \frac{1}{(1+x)^2} \Rightarrow I_1 \simeq -\frac{1}{32\pi} \ln \Lambda.$$

This defines the contribution from this part of the G^3 contraction.

The other integral corresponding to a constant prefactor of q_x^2, q_y^2 is

$$I_2 = \int_u^{+\infty} dt_1 \int_u^{+\infty} dt_2 \int_{\mathbf{q}} q_x^2 e^{-2(t_1+t_2)q^2} e^{-t_1 X} e^{-t_2 Y} \\ = -\frac{1}{16\pi} \ln \Lambda.$$

We now have to collect all these results to explicitly contract the three tensors

$$G_{iab}(k_1 - q + Q, k_2 + q - Q) G_{bcl}(q - Q, k_2) \\ G_{jca}(q - Q, k_1 - q + Q),$$

and simplify them with the results of the two above integrals. This is most conveniently done using a numerical program like *e.g* Mathematica. The resulting G^3 contribution to the G 's is embedded in the results of the next subsection.

4. Explicit RG equations

Armed with this example, one can simply repeat this procedure for each of the diagram of figure 8. The final explicit result reads, in terms of the original coefficients, the following equations. Although the only useful form of them may be a numerical routine, we include them for completeness and for the brave and bold readers.

$$\partial_l \delta c = -\frac{1}{8\pi} (g_1 - g_4)^2 + \frac{1}{8\pi} \left(-\frac{1}{2} \delta c (3g_0^2 + g_2^2 - g_1^2 + g_4^2 + 4g_1 g_4) + \frac{d}{2} (g_1 - g_4)(g_0 - g_2) \right), \\ \partial_l d = -\frac{1}{8\pi} (g_1 - g_4)^2 - \frac{1}{8\pi} \left(\frac{1}{2} \delta c (g_4^2 - g_1^2) + d(g_0^2 + g_2^2 + 2g_1 g_4 + g_0 g_4 + g_1 g_2) \right),$$

$$\partial_l g_0 = \left(-\frac{1}{4\pi} (g_0^2 + g_2^2) - \frac{1}{16\pi} (g_1 + g_4)^2 \right) g_0 + \frac{1}{32\pi} \left[14g_0^3 + \frac{5}{2}g_0g_1^2 + 2g_1^3 + g_0g_1g_2 + g_1^2g_2 + 7g_1g_2^2 + 6g_0g_1g_4 \right. \\ \left. + \frac{11}{2}g_1^2g_4 + g_0g_2g_4 + g_1g_2g_4 + 5g_2^2g_4 + \frac{7}{2}g_0g_4^2 + 5g_1g_4^2 + \frac{3}{2}g_4^3 \right],$$

$$\partial_l g_1 = \left(-\frac{1}{4\pi} (g_0^2 + g_2^2) - \frac{1}{16\pi} (g_1 + g_4)^2 \right) g_1 - \frac{1}{4\pi} (g_1 - g_4)(u_2 - u_4) + \frac{1}{2\pi} (g_1 - g_4)(w_2 - w_3) \\ + \frac{1}{32\pi} \left[8g_0^2g_1 - \frac{1}{2}g_0g_1^2 + 2g_1^3 + g_0g_1g_2 + g_1^2g_2 + 10g_0g_2^2 + 7g_1g_2^2 + 2g_0^2g_4 + 12g_0g_1g_4 \right. \\ \left. + \frac{13}{2}g_1^2g_4 + g_0g_2g_4 + g_1g_2g_4 - g_2^2g_4 + \frac{9}{2}g_0g_4^2 + 3g_1g_4^2 - \frac{3}{2}g_4^3 \right],$$

$$\partial_l g_2 = \left(-\frac{1}{4\pi} (g_0^2 + g_2^2) - \frac{1}{16\pi} (g_1 + g_4)^2 \right) g_2 + \frac{1}{32\pi} \left[-\frac{1}{2}g_0g_1^2 - 2g_0^2g_2 + 12g_0g_1g_2 + 8g_1^2g_2 + g_0g_1g_4 + \frac{3}{2}g_1^2g_4 \right. \\ \left. + 14g_0g_2g_4 + 12g_1g_2g_4 + \frac{3}{2}g_0g_4^2 + g_1g_4^2 + 8g_2g_4^2 - \frac{1}{2}g_4^3 \right],$$

$$\partial_l g_4 = \left(-\frac{1}{4\pi} (g_0^2 + g_2^2) - \frac{1}{16\pi} (g_1 + g_4)^2 \right) g_4 + \frac{1}{4\pi} (g_1 - g_4)(u_2 - u_4) - \frac{1}{2\pi} (g_1 - g_4)(w_2 - w_3) \\ + \frac{1}{32\pi} \left[\frac{19}{2}g_0g_1^2 + 2g_0^2g_2 + 2g_0g_1g_2 - 2g_1^2g_2 + 4g_0g_2^2 + 6g_1g_2^2 \right. \\ \left. + 4g_0^2g_4 + 7g_0g_1g_4 - \frac{5}{2}g_1^2g_4 + 2g_1g_2g_4 + 14g_2^2g_4 + \frac{11}{2}g_0g_4^2 + g_1g_4^2 + \frac{7}{2}g_4^3 \right],$$

$$\partial_l u_1 = \left(-\frac{3}{8\pi} (g_0^2 + g_2^2) - \frac{1}{8\pi} (g_1 + g_4)^2 \right) u_1 - \frac{1}{2\pi} (u_1^2 + u_3^2) - \frac{3}{2\pi} (w_1^2 + w_2^2) - \frac{1}{\pi} (w_1^2 + w_3^2) \\ - \frac{1}{64\pi} \left(12g_0^4 + 4g_0^2g_1^2 + 3g_1^4 + 4g_0^2g_1g_2 + 8g_0g_1g_2^2 + 3g_1^2g_2^2 + 4g_0^2g_1g_4 + 2g_0g_1^2g_4 + 6g_1^3g_4 \right. \\ \left. + 4g_0^2g_2g_4 + 4g_1^2g_2g_4 + 10g_1g_2^2g_4 + 4g_0g_1g_4^2 + 3g_1^2g_4^2 + 4g_1g_2g_4^2 + 19g_2^2g_4^2 + 2g_0g_4^3 \right),$$

$$\partial_l u_2 = \left(-\frac{3}{8\pi} (g_0^2 + g_2^2) - \frac{1}{8\pi} (g_1 + g_4)^2 \right) u_2 - \frac{1}{2\pi} (u_2^2 + u_4^2) - \frac{3}{2\pi} (2w_1w_2) - \frac{1}{\pi} (w_2^2 + w_3^2) \\ - \frac{1}{64\pi} \left(17g_0^2g_1^2 + 2g_1^3g_2 + 4g_0g_1g_2^2 + 4g_2^4 + 14g_0^2g_1g_4 + 4g_0g_1^2g_4 + 8g_0^2g_2g_4 + 4g_1^2g_2g_4 + 4g_0g_2^2g_4 \right. \\ \left. + 12g_1g_2^2g_4 + g_0^2g_4^2 + 4g_0g_1g_4^2 + g_1^2g_4^2 + 2g_1g_2g_4^2 + 12g_2^2g_4^2 + 2g_1g_4^3 + g_4^4 \right),$$

$$\partial_l u_3 = \left(-\frac{3}{8\pi} (g_0^2 + g_2^2) - \frac{1}{8\pi} (g_1 + g_4)^2 \right) u_3 - \frac{1}{2\pi} (2u_1u_3) - \frac{3}{2\pi} (2w_3^2) - \frac{1}{\pi} (2w_2w_3) \\ - \frac{1}{64\pi} \left(g_1^4 + 4g_0g_1^2g_2 + 4g_0^2g_2^2 + 28g_0g_1g_2^2 + g_1^2g_2^2 + 10g_0g_1^2g_4 + 2g_1^3g_4 + 8g_0g_1g_2g_4 + 4g_0g_2^2g_4 \right. \\ \left. + 2g_1g_2^2g_4 + 4g_0^2g_4^2 + 16g_0g_1g_4^2 + g_1^2g_4^2 + 4g_0g_2g_4^2 + g_2^2g_4^2 + 6g_0g_4^3 \right),$$

$$\partial_l u_4 = \left(-\frac{3}{8\pi} (g_0^2 + g_2^2) - \frac{1}{8\pi} (g_1 + g_4)^2 \right) u_4 - \frac{1}{2\pi} (2u_2u_4) - \frac{3}{2\pi} (2w_3^2) - \frac{1}{\pi} (2w_1w_3) \\ - \frac{1}{64\pi} \left(g_0^2g_1^2 + 12g_0^2g_1g_2 + 4g_0g_1^2g_2 + 2g_1^3g_2 + 4g_0^2g_2^2 + 4g_1^2g_2^2 + 2g_0^2g_1g_4 + 20g_0^2g_2g_4 \right. \\ \left. + 8g_0g_1g_2g_4 + 16g_1^2g_2g_4 + g_0^2g_4^2 + g_1^2g_4^2 + 4g_0g_2g_4^2 + 14g_1g_2g_4^2 + 2g_1g_4^3 + g_4^4 \right),$$

$$\begin{aligned}\partial_t v_1 = & \left(-\frac{3}{8\pi} (g_0^2 + g_2^2) - \frac{1}{8\pi} (g_1 + g_4)^2 \right) v_1 - \frac{1}{\pi} (w_1^2 + w_3^2) - \frac{1}{\pi} (u_1 v_1 + u_3 v_2) - \frac{3}{2\pi} (v_1^2 + v_2^2) \\ & - \frac{1}{64\pi} \left(12g_0^4 + 4g_0^2 g_1^2 + 3g_1^4 + 4g_0^2 g_1 g_2 + 8g_0 g_1 g_2^2 + 3g_1^2 g_2^2 + 4g_0^2 g_1 g_4 + 2g_0 g_1^2 g_4 + 6g_1^3 g_4 + 4g_0^2 g_2 g_4 \right. \\ & \left. + 4g_1^2 g_2 g_4 + 10g_1 g_2^2 g_4 + 4g_0 g_1 g_4^2 + 3g_1^2 g_4^2 + 4g_1 g_2 g_4^2 + 19g_2^2 g_4^2 + 2g_0 g_4^3 \right),\end{aligned}$$

$$\begin{aligned}\partial_t v_2 = & \left(-\frac{3}{8\pi} (g_0^2 + g_2^2) - \frac{1}{8\pi} (g_1 + g_4)^2 \right) v_2 - \frac{1}{\pi} (w_2^2 + w_3^2) - \frac{1}{\pi} (u_3 v_1 + u_1 v_2) - \frac{3}{2\pi} (2v_1 v_2) \\ & - \frac{1}{64\pi} \left(g_0^2 g_1^2 + 12g_0^2 g_1 g_2 + 4g_0 g_1^2 g_2 + 2g_1^3 g_2 + 4g_0^2 g_2^2 + 4g_1^2 g_2^2 + 2g_0^2 g_1 g_4 + 20g_0^2 g_2 g_4 + 8g_0 g_1 g_2 g_4 \right. \\ & \left. + 16g_1^2 g_2 g_4 + g_0^2 g_4^2 + g_1^2 g_4^2 + 4g_0 g_2 g_4^2 + 14g_1 g_2 g_4^2 + 2g_1 g_4^3 + g_4^4 \right),\end{aligned}$$

$$\begin{aligned}\partial_t v_3 = & \left(-\frac{3}{8\pi} (g_0^2 + g_2^2) - \frac{1}{8\pi} (g_1 + g_4)^2 \right) v_3 - \frac{1}{\pi} (w_1 w_3 + w_2 w_3) - \frac{1}{\pi} (u_2 v_3 + u_4 v_3) - \frac{3}{2\pi} 2v_3^2 \\ & - \frac{1}{64\pi} \left(\frac{17}{2} g_0^2 g_1^2 + \frac{1}{2} g_1^4 + 2g_0 g_1^2 g_2 + g_1^3 g_2 + 2g_0^2 g_2^2 + 16g_0 g_1 g_2^2 + \frac{1}{2} g_1^2 g_2^2 + 2g_2^4 + 7g_0^2 g_1 g_4 \right. \\ & \left. + 7g_0 g_1^2 g_4 + g_1^3 g_4 + 4g_0^2 g_2 g_4 + 4g_0 g_1 g_2 g_4 + 2g_1^2 g_2 g_4 + 4g_0 g_2^2 g_4 + 7g_1 g_2^2 g_4 \right. \\ & \left. + \frac{5}{2} g_0^2 g_4^2 + 10g_0 g_1 g_4^2 + g_1^2 g_4^2 + 2g_0 g_2 g_4^2 + g_1 g_2 g_4^2 + \frac{13}{2} g_2^2 g_4^2 + 3g_0 g_4^3 + g_1 g_4^3 + \frac{1}{2} g_4^4 \right),\end{aligned}$$

$$\begin{aligned}\partial_t w_1 = & \left(-\frac{3}{8\pi} (g_0^2 + g_2^2) - \frac{1}{8\pi} (g_1 + g_4)^2 \right) w_1 \\ & - \frac{1}{64\pi} \left[12g_0^4 + 4g_0^2 g_1^2 + 4g_0^2 g_1 g_2 + 4g_0 g_1^2 g_2 + 6g_1^3 g_2 + 4g_0 g_2^3 + 4g_0^2 g_1 g_4 + 2g_0 g_1^2 g_4 + 4g_0^2 g_2 g_4 + 16g_1^2 g_2 g_4 + 4g_1 g_2^2 g_4 \right. \\ & \left. + 4g_0 g_1 g_4^2 + 10g_1 g_2 g_4^2 + 16g_2^2 g_4^2 + 2g_0 g_4^3 \right] \\ & - \frac{1}{\pi} (u_1 w_1 + u_3 w_3) - \frac{1}{2\pi} (u_1 w_1 + u_3 w_2) - \frac{3}{2\pi} (v_1 w_1 + v_2 w_2) - \frac{1}{\pi} (v_1 w_1 + v_2 w_3),\end{aligned}$$

$$\begin{aligned}\partial_t w_2 = & \left(-\frac{3}{8\pi} (g_0^2 + g_2^2) - \frac{1}{8\pi} (g_1 + g_4)^2 \right) w_2 \\ & - \frac{1}{64\pi} \left[7g_0^2 g_1^2 + g_1^4 + 10g_0^2 g_1 g_2 + 2g_0 g_1^2 g_2 + 2g_0 g_1 g_2^2 + g_1^2 g_2^2 + 4g_1 g_2^3 + 8g_0^2 g_1 g_4 + 2g_0 g_1^2 g_4 + 2g_1^3 g_4 + 14g_0^2 g_2 g_4 \right. \\ & \left. + 4g_0 g_1 g_2 g_4 + 6g_1^2 g_2 g_4 + 2g_0 g_2^2 g_4 + 8g_1 g_2^2 g_4 + g_0^2 g_4^2 + 2g_0 g_1 g_4^2 + 2g_1^2 g_4^2 + 2g_0 g_2 g_4^2 + 6g_1 g_2 g_4^2 + 7g_2^2 g_4^2 + 2g_1 g_4^3 + g_4^4 \right] \\ & - \frac{1}{\pi} (u_2 w_2 + u_4 w_3) - \frac{1}{2\pi} (u_3 w_1 + u_1 w_2) - \frac{3}{2\pi} (v_2 w_1 + v_1 w_2) - \frac{1}{\pi} (v_2 w_1 + v_1 w_3),\end{aligned}$$

$$\begin{aligned}\partial_t w_3 = & \left(-\frac{3}{8\pi} (g_0^2 + g_2^2) - \frac{1}{8\pi} (g_1 + g_4)^2 \right) w_3 \\ & - \frac{1}{64\pi} \left[\frac{7}{2} g_0^2 g_1^2 + g_1^4 + 5g_0^2 g_1 g_2 + 9g_0 g_1^2 g_2 + g_1^3 g_2 + 2g_0^2 g_2^2 + 3g_0 g_1 g_2^2 + \frac{1}{2} g_1^2 g_2^2 + 6g_0 g_2^3 + 2g_1 g_2^3 + 4g_0^2 g_1 g_4 + 6g_0 g_1^2 g_4 \right. \\ & \left. + g_1^3 g_4 + 7g_0^2 g_2 g_4 + 6g_0 g_1 g_2 g_4 + 5g_1^2 g_2 g_4 + 3g_0 g_2^2 g_4 + 4g_1 g_2^2 g_4 + \frac{5}{2} g_0^2 g_4^2 + 9g_0 g_1 g_4^2 + g_1^2 g_4^2 + 3g_0 g_2 g_4^2 + 4g_1 g_2 g_4^2 \right. \\ & \left. + \frac{7}{2} g_2^2 g_4^2 + 3g_0 g_4^3 + g_1 g_4^3 + \frac{1}{2} g_4^4 \right] \\ & - \frac{1}{\pi} \frac{1}{2} (u_3 w_1 + u_4 w_2 + u_1 w_3 + u_2 w_3) - \frac{1}{2\pi} (u_2 w_3 + u_4 w_3) - \frac{3}{2\pi} (2v_3 w_3) - \frac{1}{\pi} (v_3 w_2 + v_3 w_3).\end{aligned}$$

-
- ¹ B.S. Shastry and B. Sutherland, *Physica B* **108**, 1069 (1981).
- ² C.K. Majumdar and D.K. Ghosh, *J. Math. Phys.* **10**, 1388 (1969).
- ³ Shin Miyahara and Kazuo Ueda, *Phys. Rev. Lett.* **82**, 3701 (1999)
- ⁴ E. Müller-Hatrmann, R.R.P. Singh, C. Knetter and G. Uhrig, *Phys. Rev. Lett.* **84**, 1808 (2000).
- ⁵ Akihisa Koga, Norio Kawakami, *Phys. Rev. Lett.* **84**, 4461 (2000)
- ⁶ S. Miyahara and K. Ueda, *J. Phys. Soc. Jpn.* **69** (2000).
- ⁷ H. Kageyama *et al.*, *Phys. Rev. Lett.* **82**, 3168 (1999).
- ⁸ Throughout this paper, we will use arrow notations (\vec{S}) for vector operators in the spin space, and boldface notations (\mathbf{x}) for vectors in the real space.
- ⁹ Note that the SS dimer state is thus an exact eigenstate of the 2D Heisenberg antiferromagnet (however, like the fully-polarized ferromagnetic eigenstate, it is highly excited for $J_1 = 0$).
- ¹⁰ M. Albrecht and F. Mila, *EuroPhys. Lett.* **34**, 145 (1996).
- ¹¹ M.P.A. Fisher, P.B. Weichman, G. Grinstein and D.S. Fisher, *Phys. Rev. B* **40**, 546 (1989)
- ¹² Subir Sachdev, *Quantum Phase Transitions*, Camb. Univ. Press (1999); N. Read and S. Sachdev, *Physical Review Letters* **66**, 1773 (1991); S. Sachdev and N. Read, *Int. J. of Mod. Phys. B* **5**, 219 (1991); S. Sachdev, *Phys. Rev. B* **45**, 12377 (1992).
- ¹³ P. W. Anderson, *Science* **235**, 1198 (1987); S. Kivelson, D. S. Rokhsar, and J. Sethna, *Phys. Rev.* **B35**, 8865 (1987) ; L. Balents, M.P.A. Fisher, and C. Nayak, *Phys. Rev.* **B60**, 1654 (1999); *ibid*, *Phys. Rev.* **B61**, 6307 (2000); T. Senthil and Matthew P. A. Fisher, *Phys. Rev.* **B62**, 7850 (2000).
- ¹⁴ S. Sachdev and R.N. Bhatt, *Phys. Rev. B* **41**, 9323 (1990)
- ¹⁵ We deviate slightly from Ref. 14 by not introducing redundant “singlet” operators. These were intended technically to maintain the hard-core constraint, thereby introducing an unphysical U(1) gauge symmetry. For the general coarse-grained Landau theory considerations employed here, they are unnecessary.
- ¹⁶ D. Carpentier and L. Balents, unpublished.
- ¹⁷ S. Sachdev, private communication.
- ¹⁸ J. Zinn-Justin, *Quantum field theory and critical phenomena*, Oxford (1989).
- ¹⁹ H. Lin, L. Balents and M.P.A. Fisher, *Phys. Rev. B* **56**, 6569 (1997).
- ²⁰ R. M. Konik, H. Saleur, and A. W. W. Ludwig, cond-mat/0009166.